Faculty of Mathematical Sciences

University of Twente

University for Technical and Social Sciences

P.O. Box 217
7500 AE Enschede
The Netherlands
Phone: +31-53-4893400
Fax: +31-53-4893114
Email: memo@math.utwente.nl

Memorandum No. 1555

Geometric formulation of generalized bond graph models
Part I: Generalized junction structures

G. Golo, P.C. Breedveld,[1]
B.M. Maschke[2] and A.J. van der Schaft

November 2000

ISSN 0169-2690

[1] Faculty of Electrical Engineering, University of Twente, P.O. Box 217, 7500 AE Enschede
[2] ULAGEP, CNRS-UMR, 5007-ESCPE, Universite Claude Bernard Lyon 1, France

Geometric Formulation of Generalized Bond Graph Models – Part I Generalized Junction Structures

G. Golo[1,2], P.C. Breedveld[1,3], B.M. Maschke[4], A.J. van der Schaft[1,2]

[1]Cornelis J. Drebbel Institute for Mechatronics,
[2]Faculty of Mathematical Sciences, University of Twente, P.O. Box 217, 7500 AE Enschede, Netherlands,
[3]Faculty of Electrical Engineering, University of Twente, P.O. Box 217, 7500 AE Enschede, Netherlands
[4]U LAGEP, CNRS-UMR 5007–ESCPE, Universite Claude Bernard Lyon1, France

E-mails: G.Golo@math.utwente.nl, P.C.Breedveld@el.utwente.nl, Maschke@lagep.univ-lyon1.fr, A.J.vanderSchaft@math.utwente.nl

Abstract: *This paper deals with the extraction of input-output equations that describe a generalized junction structure. This is done by associating a Dirac structure to the generalized junction structure. Since any Dirac structure admits a hybrid input-output representation, the input-output equations for the generalized junction structure can be found. The tools necessary for the manipulation of these equations are also developed. An algorithm for practical extraction of these equations is given. Also, it is analyzed when a general junction structure is singular, and an algorithm for reducing a singular generalized junction structure to a non-singular one is provided.*

Keywords: *Network modeling of physical systems, Generalized bond graphs, Dirac structures.*

Mathematics Subject Classification: *70G10, 70H45, 93A30, 93B29, 94C05.*

0. General Introduction

Bond graph theory introduced by Paynter in 1961 is a powerful and elegant way of physical system modeling [22], [13], [9]. This technique is graphically oriented and its outcome, the bond graph model, represents a multiport system involving energy flows. This approach supports one of the most important concepts in physical system theory, the concept of what Paynter calls "reticulation" and Kron "tearing". It means that it is possible to concentrate and to separate certain properties of an object and to describe that object as a system of interconnected elements [9]. The bond graph formalism used here is based on a classification of physical variables rooted in thermodynamics [10], [9]. This leads to the generalized bond graph formalism [10] based on abstraction of the elements of a network and the systematic use of a unit gyrator called symplectic gyrator. The network structure of generalized bond graph (topology of energy flow), called generalized junction structure, displays the invariants of a physical system according to Tellegen's and Kirchhoff's theorems for networks, but corresponds to an additional abstraction level [18].

This paper and its successor aim to give a *geometric formulation* of generalized bond graphs. The idea to treat generalized bond graphs in this way is not new. It has been shown before that there exists a strong relation between the geometric structures of analytical mechanics such as symplectic forms [21, 24], Poisson structures [18] and generalized junction structures. Also, it has been shown that if the generalized junction structure can be related to a Poisson structure then the generalized bond graph is related to a port controlled Hamiltonian system with dissipation [19], [29]. Here, for the first time we explicitly show that a generalized junction structure can be always related to a Dirac structure, which is a general representation of a power conserving interconnection structure of a physical system and which is treated in details in [11], [12], [30]. Based on this we also prove that a generalized bond graph can be always related to an implicit port controlled Hamiltonian system with dissipation defined in [30], [12].

The geometric treatment of generalized bond graphs is not only an elegant but also a powerful tool for the analysis of generalized bond graphs and for the derivation of equations suitable for numerical simulation. A lot of effort has been invested in solving these two problems. A thorough overview of proposed solutions can be found in [32]. A common feature of the proposed solutions is that to every port of a node of

a generalized bond graph besides the power direction two directions are associated, called effort direction and flow direction. The effort direction and the flow direction are opposite to each other and are known together as the causality of the port. A port equipped with these directions is called an augmented port. The possible causality of a port depends on the type of elements it adjoins. This leads to certain rules that have to be obeyed. The definitions of these rules and the search for procedures that assign causality to generalized bond graph, have been investigated in many papers [1], [2, 3, 4, 5], [13], [14, 15, 16], [23, 25], [26, 27], [32]. The idea of our approach is similar to the previous ones in the sense that we also want to assign causality to a generalized bond graph. However, it differs from the previous ones in the sense that it does not strive for a sequential causality assignment procedure for the assigning causality of a generalized bond graph but instead for an equivalence transformation of the generalized junction structure. Our approach is more efficient with respect to the preparation for the numerical simulation than other techniques. There are no multiple solutions and there is no need for introducing so called break variables. Also it features an easy implementation and it can be applied to any type of generalized junction structure.
Systematic procedures for constructing generalized bond graph models of physical systems lead in many cases to generalized bond graph models containing dependent states. Although the simulation of a generalized bond graph model containing dependent states can be carried out by means of implicit numerical techniques [32], the computational burden is significantly increased. We propose methods for the elimination of dependent states in a generalized bond graph model. We also investigate existence of dynamic invariants in generalized bond graphs. In general, generalized bond graphs containing dynamic invariants but no dependent states can be simulated by means of explicit numerical techniques. However, the existence of dynamic invariants should be explicitly taken into account in order to avoid an eventual increase of inaccuracy of the numerical simulations. We propose a method for the elimination of dynamic invariants.

1. Introduction

It has often been observed that the finding of an appropriate description of a generalized junction structure is the main problem for the analysis of a generalized bond graph and for the extraction of equations suitable for numerical simulation.

This paper deals with the extraction of input-output equations describing a generalized junction structure. Also, the tools necessary for manipulation of these equations are developed. The idea for the method of extraction of these equations is based on the fact that a Dirac structure can be related to the generalized junction structure. Since a Dirac structure admits a hybrid input-output representation, the desired equations are found.

This paper is organized in the following way. In section 2, the definitions of generalized bond graphs and generalized junction structures are recalled. Also the classification of ports according to the type and to the invertibility of constitutive relations is explained. In Section 3 the definitions of constant Dirac structures and Dirac structures on a differentiable manifold are recalled. The various representations of Dirac structures in terms of some structural matrices are presented. An equivalence relation between Dirac structures is proposed, and the result concerning the compositionality properties of Dirac structures is recalled. In section 4 the main result of this paper is presented. In subsection 4.1, it is proved that a Dirac structure can be always related to a generalized junction structure. How that can be done in a practical way is shown in section 4.2. Also, the tools for manipulation of equations describing a generalized junction structure are developed. Finally, singular generalized junction structures are defined, and sufficient and necessary conditions for a generalized junction structure not being singular are given.

Notation

E - set of power discontinuous elements (storage multiports (C), dissipative multiports (R) and sources (Se, Sf)).

Ξ, Ξ^0, Ξ^1- set of junctions, set of 0-junctions, set of 1-junctions, respectively.

χ, χ^0, χ^1 - an element of the set Ξ,Ξ^0, Ξ^1, respectively.

T, T^{TF}, T^{GY} - set of transducers, set of transformers, set of gyrators, respectively.

τ, τ^{TF}, τ^{GY} - an element of the set T,T^{TF}, T^{GY}, respectively.

B - set of bonds.

β - an element of the set B.

Π - set of ports.

π - an element of the set Π.

$\mathcal{R}$ - set of real numbers.

$\mathcal{N}$ - set of natural numbers.

2. Generalized Bond Graphs, Generalized Junction Structure

This section starts with recalling the definition of generalized bond graphs as the general structure of power continuous interconnection in bond graph models [9], [7], [10], [8]. The notation that will be used in the sequel concerning the classification of elements and ports is introduced.

2.1. Generalized Bond Graph

The basic idea behind the **G**eneralized **B**ond **G**raph (GBG) framework is the decomposition of conventional physical domains (e.g. mechanical or electrical), which have two types of storage, into new domains, which have only one type of storage (e.g., the mechanical domain is decomposed into a kinetic and a potential domain) [9]. A generic generalized bond graph is shown in Figure 1. Here, $\mathbb{C}$, stands for the collection of C-multiports, $\mathbb{R}$ stands for the collection of dissipative multiports, $\mathbb{Se}$ stands for the collection of effort sources, $\mathbb{Sf}$ stands for the collection of flow sources and $\mathbb{GJS}$ stands for **G**eneralized **J**unction **S**tructure (GJS). The generalized junction structure is composed of the following elements: junctions (0-junction, 1-junction) and transducers (transformer and gyrator).

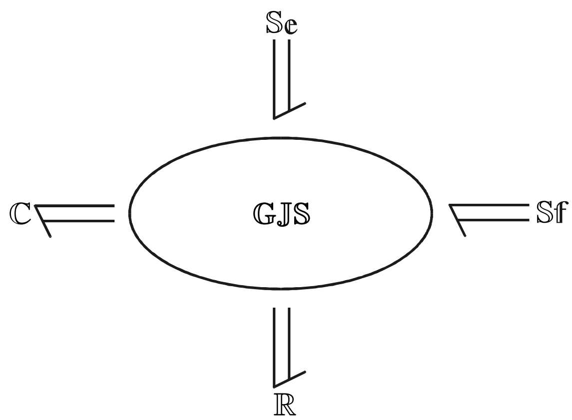

Figure 1: Generic generalized bond graph

Some definitions regarding basic links are given below.

Definition 1 (*P-link*)

A P-link is a path of length one between two junctions.

Definition 2 (*TF-link*)

A TF-link is a path of length two between two junctions via a transformer.

Definition 3 (*GY-link*)

A GY-link is a path of length two between two junctions via a gyrator.

Definition 4 (*Basic links*)

A basic link is a link that is either P-link or TF-link or GY-link.

Definition 5 (*Direct connection*)

Two junctions are directly connected if there is a basic link between them.

Now we give the definition of the class of generalized bond graphs considered here.

Assumption 1 (*Class of GBG*)

The class of generalized bond graphs considered here satisfies the following conditions:

[As1a] *Every bond always joins at least one junction.*

[As1b] *The number of parallel basic links between any two junctions is smaller or equal than one.*

[As1c] *The vertices of a P-link are always different types of junctions.*

[As1d] *No basic link of GBG joins a junction to itself.*

[As1e] *The transducers can be modulated only by the states of storage multiports.*

[As1f] *The ratio of a modulated transducer is a smooth function of the states of storage multiports.*

Remark 1 (*Class of GBG*)

If a GBG does not satisfy any of [As1a]-[As1d] then it can be transformed into a GBG satisfying those conditions by using basic equivalence operations [22], [14], [17], [9], [7]. The condition [As1e] ensures that the ambiguity of internal modulation of transformers and gyrators is avoided (see [9], pp. 26). In this way the principle of modularity is also preserved.

2.2. Generalized junction structure

The part of a generalized bond graph that contains topological information is known as the generalized junction structure. The generalized junction structure is composed of all power continuous, non-entropic multiport elements such as junctions and transducers [9].

A pictorial representation of a generalized junction structure with ports denoted with $\boldsymbol{\pi}$ (without orientation) is shown in Figure 2. The ports represent the connections of the GJS to the power discontinuous multiports. Also, since the condition [As1a] is satisfied a port always joins a junction.

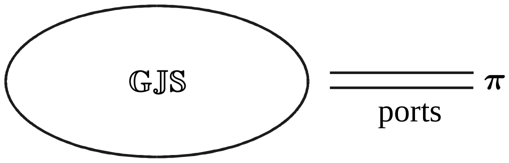

Figure 2: Generic generalized junction structure

With any bond two power variables are associated the flow and its dual (conjugate) variable the effort. Below, the definitions of port variables and internal variables are given.

Definition 6 (*Port variables*)

Port variables are power variables associated with port $\boldsymbol{\pi}$.

Definition 7 (*Internal variables*)

Internal variables are power variables associated with bond that does not join power discontinuous elements.

Since the port variables denoted by $\boldsymbol{f}$ (flow) and $\boldsymbol{e}$ (effort) are dual variables, we can define the duality product $\langle \boldsymbol{e} \mid \boldsymbol{f} \rangle$ as the representation of power. The duality product is given by

$$\langle \boldsymbol{e} \mid \boldsymbol{f} \rangle = \sum_{i=1}^{n} \sigma_{\pi}\left(\pi_i, \chi_i\right) f_i e_i \; . \tag{1}$$

Here, n is the number of the ports, f_i, e_i are the power variables of π_i, and χ_i, π_i are incident. The definition of the function σ_{π} is as follows (π, η are incident)

$$\sigma_{\pi}\left(\pi, \eta\right) = \begin{cases} 1, \text{if } \pi \text{ is outgoing in } \eta \\ -1, \text{if } \pi \text{ is incoming in } \eta \end{cases}.$$

Let $\boldsymbol{f}_{\text{out}}, \boldsymbol{e}_{\text{out}}$ represent the power variables of the ports leaving in a GJS, and let $\boldsymbol{f}_{\text{in}}, \boldsymbol{e}_{\text{in}}$ represent the power variables of ports entering in the GJS. Then (1) can be rewritten as

$$P = \langle \boldsymbol{e} \mid \boldsymbol{f} \rangle = P_{\text{out}} - P_{\text{in}} = \boldsymbol{e}_{\text{out}}^{\text{T}} \boldsymbol{f}_{\text{out}} - \boldsymbol{e}_{\text{in}}^{\text{T}} \boldsymbol{f}_{\text{in}} \; .$$

Therefore, the duality product represents the difference between the outgoing power and the incoming power.

The main feature of the GJS is power continuity, i.e. a zero power balance at its port, that is $\langle \boldsymbol{e} \mid \boldsymbol{f} \rangle = 0$. Therefore, the GJS relates the flows, $\boldsymbol{f}$, and the efforts, $\boldsymbol{e}$, of the ports to each other. Those relations will be called interconnection relations. In section 4 is shown how the interconnection relations can be practically determined.

Let us consider a GJS such that the port π_i is entering in the GJS and it joins a 0-junction, Figure $3a$, or it joins a 1-junction, Figure $3b$. Then it can be replaced by $\overline{\pi}_i$ that is outgoing with respect to the GJS as shown in Figure $3c$, respectively, Figure $3d$. Thus, we can assume that all ports are outgoing with respect to GJS. As a result, we can assume that the duality product is given by

$$\langle \boldsymbol{e} \mid \boldsymbol{f} \rangle = \boldsymbol{e}^{\mathrm{T}} \boldsymbol{f} .$$

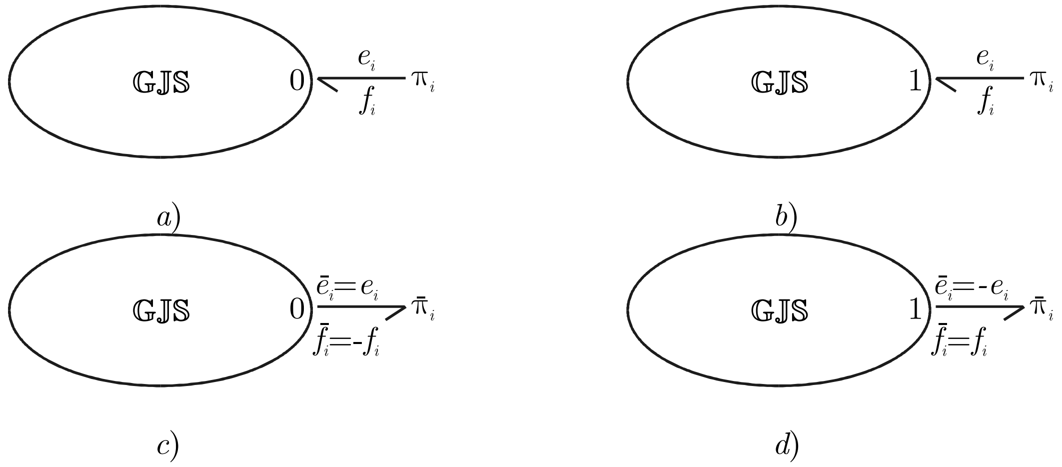

Figure 3: Changing the direction of ports

Consider a generalized junction structure together with the ports $\boldsymbol{\pi}_1$ and $\boldsymbol{\pi}_2$ as shown in Figure $4a$. The combination $\boldsymbol{\pi}_1$—$\mathbb{SGY}$—bond—$\mathbb{SGY}$—bond replaces $\boldsymbol{\pi}_1$ as shown in Figure $4b$. Here, $\mathbb{SGY}$ stands for the symplectic gyrator (see e.g. [9], pp. 52). The part encircled by the dotted line represents a new generalized junction structure with ports $\bar{\boldsymbol{\pi}}_1$ and $\boldsymbol{\pi}_2$ (Figure $4c$). Therefore, the effort, respectively, the flow of $\boldsymbol{\pi}_1$ is equal to the flow, respectively, the effort of $\bar{\boldsymbol{\pi}}_1$. This procedure is called the partial dualization procedure applied to $\boldsymbol{\pi}_1$ (see [9], pp. 11).

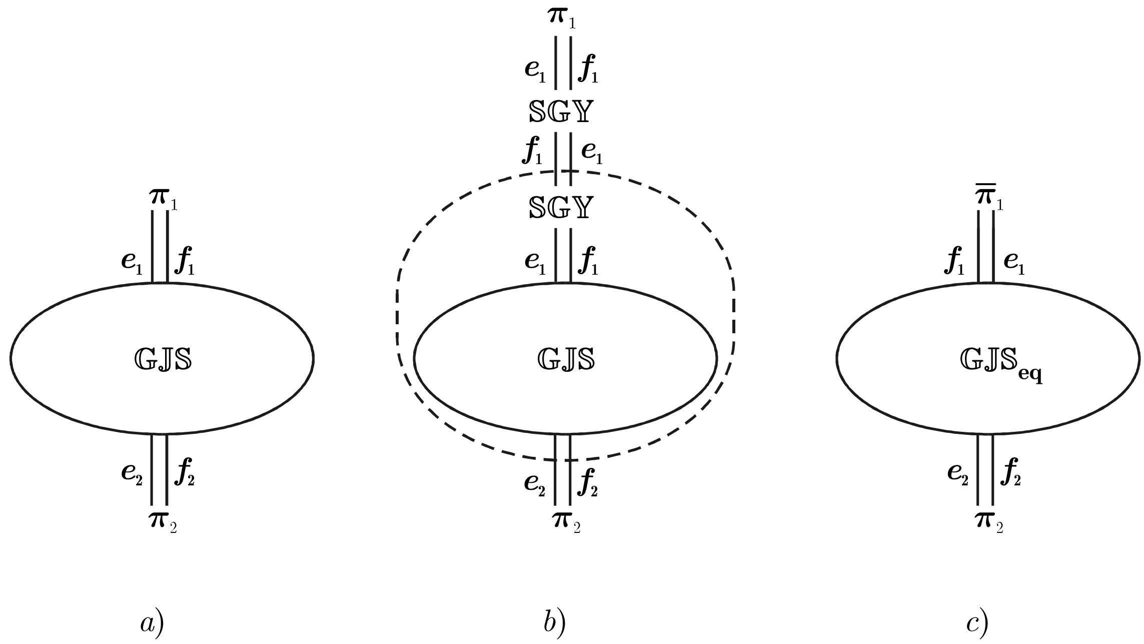

Figure 4: Partial dualization procedure applied to port $\boldsymbol{\pi}_1$

2.3. Classification of ports

Consider a port, π, and its associated power variables f, e. Let

$$\Phi(f, e, \boldsymbol{X}) = 0\,, \tag{2}$$

denote a relation between e and f imposed by a power discontinuous element (hereafter this relation will be called constitutive relation). Here $\boldsymbol{X}$ contains all other power variables and the states of C-multiports (energy variables). The port can be classified in two ways: according to the type of the constitutive relation and according to the invertibility of the constitutive relation.

According to the *type* of the constitutive relations the set of ports Π is split as

$$\Pi = \Pi^{\mathrm{Se}} \cup \Pi^{\mathrm{C}} \cup \Pi^{\mathrm{R}} \cup \Pi^{\mathrm{Sf}}\,.$$

If π represents the connection to Se- multiport, then $\pi \in \Pi^{\mathrm{Se}}$, and similarly for $\Pi^{\mathrm{C}}, \Pi^{\mathrm{R}}, \Pi^{\mathrm{Sf}}$.

According to the *invertibility* of the constitutive relations Π is split as

$$\Pi = \Pi^{\mathrm{FE}} \cup \Pi^{\mathrm{DE}} \cup \Pi^{\mathrm{A}} \cup \Pi^{\mathrm{FF}}\,.$$

Here, FF, FE, DE, A are abbreviations for **F**ixed **F**low, **F**ixed **E**ffort, **P**referred **E**ffort and **A**rbitrary, respectively. The definition of the sets $\Pi^{\mathrm{FE}}, \Pi^{\mathrm{DE}}, \Pi^{\mathrm{A}}, \Pi^{\mathrm{FF}}$ is given in Table 1.

Table 1 (*Classification of ports according to the invertibility of the constitutive relations*)

The equation (2) is solvable for f	The equation (2) is solvable for e	f is preferred to be output	e is preferred to be output	
Yes	No	/	/	$\pi \in \Pi^{\mathrm{FF}}$
No	Yes	/	/	$\pi \in \Pi^{\mathrm{FE}}$
Yes	Yes	No	Yes	$\pi \in \Pi^{\mathrm{DE}}$
Yes	Yes	No	No	$\pi \in \Pi^{\mathrm{A}}$

3. Dirac Structures

In this section we recall the definition of a Dirac structure as a general representation of a power conserving interconnection structure of a physical system. Firstly, the definition of a constant Dirac structure on a finite-dimensional linear space [11], [30] is recalled. This definition is extended to the non-linear case as explained in [30]. We also recall different kinds of representations of Dirac structures [6], [12], [29], [28]. These representations of Dirac structures are given in terms of some structural matrices. Afterward, we present a notation of equivalence between Dirac structures, which will be the basis for the transformation of a generalized junction structure presented in the next sections. Finally, the results concerning compositionality properties of Dirac structures are recalled [28].

3.1. Definitions and some properties

We start with the space of power variables $\mathcal{V}\times\mathcal{V}^*$, for some finite-dimensional linear space $\mathcal{V}$, with the power defined by

$$P=\langle \boldsymbol{e}\mid \boldsymbol{f}\rangle,\ (\boldsymbol{e},\boldsymbol{f})\in\mathcal{V}\times\mathcal{V}^*,$$

where $\langle \boldsymbol{e}\mid \boldsymbol{f}\rangle$ denotes the duality product. We call $\mathcal{V}$ the space of *flows f*, and the dual space $\mathcal{V}^*$ the space of *efforts e*. Closely related to the definition of power there exist a canonically defined bilinear form $\ll,\gg$ on the space of power variables $\mathcal{V}\times\mathcal{V}^*$, defined as

$$\ll(\boldsymbol{f}^a,\boldsymbol{e}^a),(\boldsymbol{f}^b,\boldsymbol{e}^b)\gg:=\langle \boldsymbol{e}^a\mid \boldsymbol{f}^b\rangle+\langle \boldsymbol{e}^b\mid \boldsymbol{f}^a\rangle.$$

Definition 8 [11] (*Definition of constant Dirac structure*)

A constant Dirac structure on a linear space $\mathcal{V}$ is a subspace

$$\mathcal{D}\subset\mathcal{V}\times\mathcal{V}^*$$

such that $\mathcal{D}=\mathcal{D}^{\perp}$, where $\perp$ denotes orthogonal complement with respect to the bilinear form $\ll,\gg$. In other words,

$$\mathcal{D}=\left\{(f,e)\in\mathcal{V}\times\mathcal{V}^*\mid\ll(f^a,e^a),(f^b,e^b)\gg=0,\forall(f^a,e^a),(f^b,e^b)\in\mathcal{D}\right\},\tag{3}$$

and $\mathcal{D}$ is of maximal dimension with property (3).

It can be easily shown that necessarily $\dim(\mathcal{D})=\dim(\mathcal{V})$. Furthermore, using the linearity, it can be seen [30] that $\mathcal{D}\subset\mathcal{V}\times\mathcal{V}^*$ is a Dirac structure if and only if

$$\mathcal{D}=\left\{(f,e)\in\mathcal{V}\times\mathcal{V}^*:\langle e\mid f\rangle=0\ \forall(f,e)\in\mathcal{D}\right\},\tag{4}$$

and $\mathcal{D}$ is of maximal dimension with property (4).

Dirac structures on manifolds (non-constant case) are defined as follows [30]. Let $\mathcal{Z}$ be a differentiable manifold with tangent bundle $T\mathcal{Z}$ and cotangent bundle $T^*\mathcal{Z}$. We define $T\mathcal{Z}\oplus T^*\mathcal{Z}$ as the smooth vector bundle over $\mathcal{Z}$ with the fiber at each $\boldsymbol{z}\in\mathcal{Z}$ given by $T_z\mathcal{Z}\times T_z^*\mathcal{Z}$ (see [20] pp. 42, 62, 426, 428 for the definition of tangent, cotangent and vector bundle as well as fiber).

Definition 9 [30] (*Definition of Dirac structure on differentiable manifold*)

A Dirac structure on a differentiable manifold $\mathcal{Z}$ is given by a smooth vector subbundle $\mathcal{D}\subset T\mathcal{Z}\oplus T\mathcal{Z}^*$ such that the linear space $\mathcal{D}(\boldsymbol{z})\subset T_z\mathcal{Z}\times T_z^*\mathcal{Z}$ is a Dirac *structure (in the sense of the Definition* 8*) on* $T_z\mathcal{Z}$ *, for every* $\boldsymbol{z} \in \mathcal{Z}$ *.*

Define the following subbundles of the tangent bundle, respectively cotangent bundle

$$
\begin{gathered}
\mathcal{G}_0(\boldsymbol{z}) = \left\{ \boldsymbol{f} \in T_z\mathcal{Z} : (\boldsymbol{f}, 0) \in \mathcal{D}(\boldsymbol{z}) \right\}, \\
\mathcal{G}_1(\boldsymbol{z}) = \left\{ \boldsymbol{f} \in T_z\mathcal{Z} : \exists \boldsymbol{e} \in T_z^*\mathcal{Z} \text{ s.t.} (\boldsymbol{f}, \boldsymbol{e}) \in \mathcal{D}(\boldsymbol{z}) \right\}, \\
\mathcal{P}_0(\boldsymbol{z}) = \left\{ \boldsymbol{e} \in T_z^*\mathcal{Z} : (0, \boldsymbol{e}) \in \mathcal{D}(\boldsymbol{z}) \right\}, \\
\mathcal{P}_1(\boldsymbol{z}) = \left\{ \boldsymbol{e} \in T_z^*\mathcal{Z} : \exists \boldsymbol{e} \in T_z\mathcal{Z} \text{ s.t.} (\boldsymbol{f}, \boldsymbol{e}) \in \mathcal{D}(\boldsymbol{z}) \right\}.
\end{gathered}
$$

Here, $\mathcal{G}_1(\boldsymbol{z})$ represents the set of admissible flows at the point $\boldsymbol{z}$. Similarly, $\mathcal{P}_1(\boldsymbol{z})$ represents the set of admissible efforts at the point $\boldsymbol{z}$. It can be shown ([12]) that $\mathcal{G}_0(\boldsymbol{z}) = \ker\left(\mathcal{P}_1(\boldsymbol{z})\right)$, $\mathcal{P}_0(\boldsymbol{z}) = \operatorname{ann}\left(\mathcal{G}_1(\boldsymbol{z})\right)$ and $\mathcal{P}_1(\boldsymbol{z}) = \operatorname{ann}\left(\mathcal{G}_0(\boldsymbol{z})\right)$, $\mathcal{G}_1(\boldsymbol{z}) = \ker\left(\mathcal{P}_0(\boldsymbol{z})\right)$. We assume that $\mathcal{Z}$ is given as $\mathcal{Z}=\mathcal{X} \times \mathcal{Y}$, with $\mathcal{X}$ a differentiable manifold and $\mathcal{Y}$ a linear space. Using the linearity of $\mathcal{Y}$ it follows that $T_z\mathcal{Z}$ can be identified with $T_z\mathcal{Z} = T_x\mathcal{X} \oplus \mathcal{Y}$, with $\boldsymbol{x}$ the projection of $\boldsymbol{z}$ on $\mathcal{X}$. Furthermore, we assume throughout that the Dirac structures defined on $\mathcal{Z}$ depend only on $\boldsymbol{x} \in \mathcal{X}$, i.e. $\mathcal{D}(\boldsymbol{z}) = \mathcal{D}(\boldsymbol{x})$ $\forall(\boldsymbol{x}, \boldsymbol{y}) \in \mathcal{Z}$, $\boldsymbol{x} \in \mathcal{X}$, $\boldsymbol{y} \in \mathcal{Y}$. This specific form of Dirac structures is of a great importance. As we shall see later, the manifold $\mathcal{X}$ is associated with the space of energy variables (the states of C-multiports), and the linear vector space $\mathcal{Y}$ is identified as the flow space of the ports representing the connections to the resistive multiports and the source multiports. Since we assume condition [As1e] it is clear why $\mathcal{D}$ depends only on $\boldsymbol{x}$. (We like to stress that $\mathcal{Z}$ can not be seen as a state space. Otherwise it would mean that one could associate state variables to the ports representing the connections to R-multiports).

In the previous part of this section we assumed that $\langle \boldsymbol{e} \mid \boldsymbol{f} \rangle$ represents the outgoing power. Of course, we can easily imagine situations where some of the ports of the interconnection structure are incoming ones. Denote the power variables of incoming ports by $\left(\boldsymbol{f}_{\text{in}}, \boldsymbol{e}_{\text{in}}\right) \in \mathcal{V}_{\text{in}} \times \mathcal{V}_{\text{in}}^*$ and power variables of outgoing ports by $\left(\boldsymbol{f}_{\text{out}}, \boldsymbol{e}_{\text{out}}\right) \in \mathcal{V}_{\text{out}} \times \mathcal{V}_{\text{out}}^*$. It is clear that $\mathcal{V}=\mathcal{V}_{\text{in}} \oplus \mathcal{V}_{\text{out}}$. Then the bilinear form is modified to

$$
\begin{gathered}
\ll \left(\boldsymbol{f}_{\text{out}}^a, \boldsymbol{f}_{\text{in}}^a, \boldsymbol{e}_{\text{out}}^a, \boldsymbol{e}_{\text{in}}^a\right), \left(\boldsymbol{f}_{\text{out}}^b, \boldsymbol{f}_{\text{in}}^b, \boldsymbol{e}_{\text{out}}^b, \boldsymbol{e}_{\text{in}}^b\right) \gg := \\
\left\langle \boldsymbol{e}_{\text{out}}^a \mid \boldsymbol{f}_{\text{out}}^b \right\rangle + \left\langle \boldsymbol{e}_{\text{out}}^b \mid \boldsymbol{f}_{\text{out}}^a \right\rangle - \left\langle \boldsymbol{e}_{\text{in}}^a \mid \boldsymbol{f}_{\text{in}}^b \right\rangle - \left\langle \boldsymbol{e}_{\text{in}}^b \mid \boldsymbol{f}_{\text{in}}^a \right\rangle
\end{gathered}. \tag{5}
$$

A constant respectively, non-constant Dirac structure is now defined as in Definition 8, respectively Definition 9, where the bilinear form is given by (5).

3.2. Various representations of Dirac structures

In the previous sub-section we have given the definitions and the constitutive properties of a Dirac structure. In this section we recall different kinds of representations of Dirac structures. These representations are given in terms of some structural matrices.

3.2.1. Kernel representation [12], [29]

Locally about every point $(\boldsymbol{x},\boldsymbol{y})$ in $\mathcal{Z}=\mathcal{X}\times\mathcal{Y}$, we may find $n\times n$ (n is the dimension of the manifold $\mathcal{Z}$) matrices $\boldsymbol{E}(\boldsymbol{x})$ and $\boldsymbol{F}(\boldsymbol{x})$ depending smoothly on $\boldsymbol{x}$, such that locally

$$\mathcal{D}(\boldsymbol{x})=\left\{(\boldsymbol{f},\boldsymbol{e})\in T_{\boldsymbol{z}}\mathcal{Z}\times T_{\boldsymbol{z}}^{*}\mathcal{Z}:\boldsymbol{F}(\boldsymbol{x})\boldsymbol{f}+\boldsymbol{E}(\boldsymbol{x})\boldsymbol{e}=0\right\},$$

Here, the matrices $\boldsymbol{E}(\boldsymbol{x})$ and $\boldsymbol{F}(\boldsymbol{x})$ satisfy the following conditions

$$\operatorname{rank}\left[\boldsymbol{F}(\boldsymbol{x}) \;\vdots\; \boldsymbol{E}(\boldsymbol{x})\right]=n \tag{6}$$

$$\boldsymbol{E}(\boldsymbol{x})\boldsymbol{F}^{\mathrm{T}}(\boldsymbol{x})+\boldsymbol{F}(\boldsymbol{x})\boldsymbol{E}^{\mathrm{T}}(\boldsymbol{x})=0\,. \tag{7}$$

This representation is called a kernel representation.

Again we have assumed that all ports are outgoing. If this is not the case then the kernel representation is given by

$$\begin{aligned}\mathcal{D}(\boldsymbol{x})=\Big\{&\left(\boldsymbol{f}_{\mathrm{in}},\boldsymbol{f}_{\mathrm{out}},\boldsymbol{e}_{\mathrm{in}},\boldsymbol{e}_{\mathrm{out}}\right)\in T_{\boldsymbol{z}}\mathcal{Z}\times T_{\boldsymbol{z}}^{*}\mathcal{Z}:\\ &\boldsymbol{F}_{\mathrm{in}}(\boldsymbol{x})\boldsymbol{f}_{\mathrm{in}}+\boldsymbol{E}_{\mathrm{in}}(\boldsymbol{x})\boldsymbol{e}_{\mathrm{in}}+\boldsymbol{F}_{\mathrm{out}}(\boldsymbol{x})\boldsymbol{f}_{\mathrm{out}}+\boldsymbol{E}_{\mathrm{out}}(\boldsymbol{x})\boldsymbol{e}_{\mathrm{out}}=0\Big\}.\end{aligned}$$

where, the corresponding matrices satisfy the following conditions

$$\operatorname{rank}\left[\boldsymbol{F}_{\mathrm{in}}(\boldsymbol{x}) \;\vdots\; \boldsymbol{F}_{\mathrm{out}}(\boldsymbol{x}) \;\vdots\; \boldsymbol{E}_{\mathrm{in}}(\boldsymbol{x}) \;\vdots\; \boldsymbol{E}_{\mathrm{out}}(\boldsymbol{x})\right]=n\,, \tag{8}$$

$$\boldsymbol{E}_{\mathrm{out}}(\boldsymbol{x})\boldsymbol{F}_{\mathrm{out}}^{\mathrm{T}}(\boldsymbol{x})+\boldsymbol{F}_{\mathrm{out}}(\boldsymbol{x})\boldsymbol{E}_{\mathrm{out}}^{\mathrm{T}}(\boldsymbol{x})-\boldsymbol{E}_{\mathrm{in}}(\boldsymbol{x})\boldsymbol{F}_{\mathrm{in}}^{\mathrm{T}}(\boldsymbol{x})-\boldsymbol{F}_{\mathrm{in}}(\boldsymbol{x})\boldsymbol{E}_{\mathrm{in}}^{\mathrm{T}}(\boldsymbol{x})=0\,. \tag{9}$$

Example 1 (*Electrical circuit*)

Consider the electrical circuit shown in Figure 5a. The generalized bond graph model for this system is represented in Figure 5b.

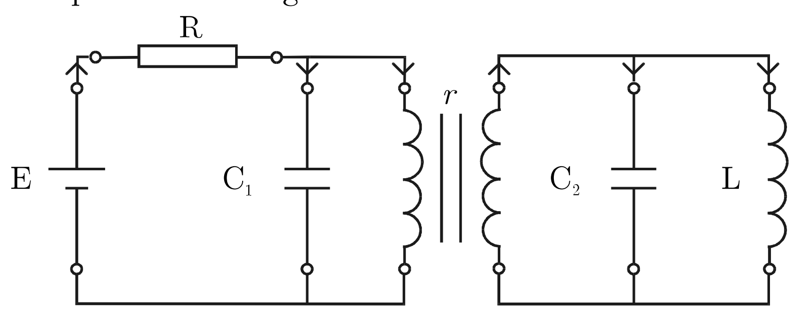

a)

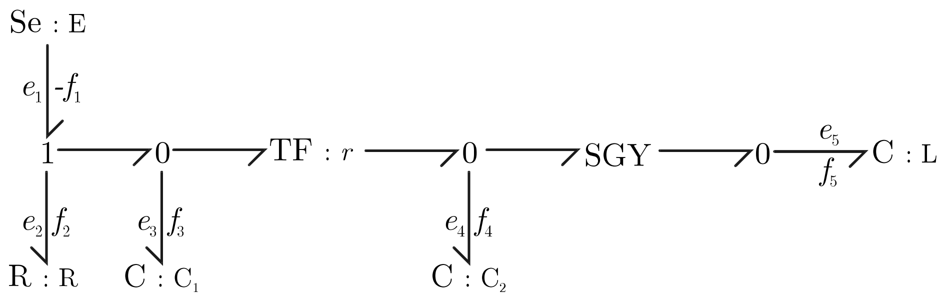

b)

Figure 5: a) Electrical circuit, b) bond graph model

The interconnection relations are given by Kirchhoff's laws and by the constitutive relations for the transformer and the symplectic gyrator, that is, $0 = -e_1 + e_2 + e_3$, $0 = e_3 - re_4$, $0 = e_4 - f_5$, $0 = f_1 + f_2$ and $0 = -r\left(f_2 - f_3\right) + e_5 + f_4$. Therefore, a matrix representation of the interconnection relations is given by

$$\underbrace{\begin{bmatrix} 1 & -1 & -1 & 0 & 0 \\ 0 & 0 & 1 & -r & 0 \\ 0 & 0 & 0 & 1 & 0 \\ 0 & 0 & 0 & 0 & 0 \\ 0 & 0 & 0 & 0 & 1 \end{bmatrix}}_{\boldsymbol{E}} \underbrace{\begin{bmatrix} e_1 \\ e_2 \\ e_3 \\ e_4 \\ e_5 \end{bmatrix}}_{\boldsymbol{e}} + \underbrace{\begin{bmatrix} 0 & 0 & 0 & 0 & 0 \\ 0 & 0 & 0 & 0 & 0 \\ 0 & 0 & 0 & 0 & -1 \\ 1 & 1 & 0 & 0 & 0 \\ 0 & -r & r & 1 & 0 \end{bmatrix}}_{\boldsymbol{F}} \underbrace{\begin{bmatrix} f_1 \\ f_2 \\ f_3 \\ f_4 \\ f_5 \end{bmatrix}}_{\boldsymbol{f}} = 0$$

A straightforward computation shows that $\operatorname{rank}\left[\boldsymbol{E} \mid \boldsymbol{F}\right] = 5$ and $\boldsymbol{E}\boldsymbol{F}^{\mathrm{T}} + \boldsymbol{F}\boldsymbol{E}^{\mathrm{T}} = 0$. Note that to obtain the interconnection relations the Se-port has been transformed as shown in Figure 3d.

3.2.2. Hybrid input-output representation [6], [28]

Suppose that $\boldsymbol{e}$ and $\boldsymbol{f}$ are split as $\begin{bmatrix} \boldsymbol{e}_1 \\ \hdashline \boldsymbol{e}_2 \end{bmatrix}$, $\begin{bmatrix} \boldsymbol{f}_1 \\ \hdashline \boldsymbol{f}_2 \end{bmatrix}$. The dimensions of the vectors $\boldsymbol{e}_1$, $\boldsymbol{e}_2$ are n_1, n_2, respectively, with $n_1 + n_2 = n$. Corresponding to these splitting, the $n \times n$ dimensional matrices $\boldsymbol{E}(\boldsymbol{x})$ and $\boldsymbol{F}(\boldsymbol{x})$ are split as $\left[\boldsymbol{E}_1(\boldsymbol{x}) \mid \boldsymbol{E}_2(\boldsymbol{x})\right]$, $\left[\boldsymbol{F}_1(\boldsymbol{x}) \mid \boldsymbol{F}_2(\boldsymbol{x})\right]$, with the dimensions of the matrices $\boldsymbol{F}_i(\boldsymbol{x}), \boldsymbol{E}_i(\boldsymbol{x})$, i=1,2 being equal. Suppose now that $\operatorname{rank}\left[\boldsymbol{E}_1(\boldsymbol{x}) \mid \boldsymbol{F}_2(\boldsymbol{x})\right] = n$. Then the Dirac structure is also given by

$$\mathcal{D}(\boldsymbol{x}) = \left\{ (\boldsymbol{f}, \boldsymbol{e}) \in T_z\mathcal{Z} \times T_z^*\mathcal{Z} : \begin{bmatrix} \boldsymbol{e}_1 \\ \hdashline \boldsymbol{f}_2 \end{bmatrix} = -\underbrace{\left[\begin{array}{c:c} \boldsymbol{J}_{11}(\boldsymbol{x}) & \boldsymbol{J}_{21}^{\mathrm{T}}(\boldsymbol{x}) \\ \hdashline -\boldsymbol{J}_{21}(\boldsymbol{x}) & \boldsymbol{J}_{22}(\boldsymbol{x}) \end{array}\right]}_{\boldsymbol{J}(\boldsymbol{x})} \begin{bmatrix} \boldsymbol{f}_1 \\ \hdashline \boldsymbol{e}_2 \end{bmatrix} \right\}, \tag{10}$$

where:

$$\boldsymbol{J}(\boldsymbol{x}) = -\boldsymbol{J}^{\mathrm{T}}(\boldsymbol{x}) = \left[\boldsymbol{E}_1(\boldsymbol{x}) \mid \boldsymbol{F}_2(\boldsymbol{x})\right]^{-1}\left[\boldsymbol{F}_1(\boldsymbol{x}) \mid \boldsymbol{E}_2(\boldsymbol{x})\right]. \tag{11}$$

The representation described by (10), (11) is called a hybrid input-output representation. Note that the definition of this representation is more general than one given in [6], [28] since we do not require that $\operatorname{rank}\left[\boldsymbol{E}_1(\boldsymbol{x})\right] = \operatorname{rank}[\boldsymbol{E}(\boldsymbol{x})]$. On the other hand, if $\operatorname{rank}\left[\boldsymbol{E}_1(\boldsymbol{x})\right] = \operatorname{rank}[\boldsymbol{E}(\boldsymbol{x})]$, then it has been shown in [6] that $\operatorname{rank}\left[\boldsymbol{E}_1(\boldsymbol{x}) \mid \boldsymbol{F}_2(\boldsymbol{x})\right] = n$.

Conversely, a Dirac structure described by (10) has the kernel representation

$$\mathcal{D}(\boldsymbol{x}) = \left\{(\boldsymbol{f},\boldsymbol{e}) \in T_{\boldsymbol{z}}\mathcal{Z} \times T_{\boldsymbol{z}}^{*}\mathcal{Z} : \underbrace{\left[\begin{array}{c:c:c:c} \boldsymbol{I}_{n_1} & \boldsymbol{J}_{21}^{\mathrm{T}}(\boldsymbol{x}) & \boldsymbol{J}_{11}(\boldsymbol{x}) & 0 \\ \hdashline 0 & \boldsymbol{J}_{22}(\boldsymbol{x}) & -\boldsymbol{J}_{21}(\boldsymbol{x}) & I_{n_2} \end{array}\right]}_{\boldsymbol{W}(\boldsymbol{x})} \left[\begin{array}{c} \boldsymbol{e}_1 \\ \hdashline \boldsymbol{e}_2 \\ \hdashline \boldsymbol{f}_1 \\ \hdashline \boldsymbol{f}_2 \end{array}\right] = 0 \right\}. \tag{12}$$

For the latter use we define $\boldsymbol{J}(\boldsymbol{x})$ and the integers n_1, n_2 to uniquely determine the matrix $\boldsymbol{W}(\boldsymbol{x})$ as

$$\boldsymbol{W}(\boldsymbol{x}) = \Theta\left(\boldsymbol{J}(\boldsymbol{x}), n_1, n_2\right) = \left[\begin{array}{c:c:c:c} \boldsymbol{I}_{n_1} & \boldsymbol{J}_{21}^{\mathrm{T}}(\boldsymbol{x}) & \boldsymbol{J}_{11}(\boldsymbol{x}) & 0 \\ \hdashline 0 & \boldsymbol{J}_{22}(\boldsymbol{x}) & \boldsymbol{J}_{21}(\boldsymbol{x}) & I_{n_2} \end{array}\right].$$

Example 2 (*Continuation of Example 1*)

Let the matrix $\boldsymbol{E}_1$ contain the 1st, 3rd, 4th, and 5th column of $\boldsymbol{E}$. Then the matrix $\boldsymbol{F}_2$ contains the 2nd column of $\boldsymbol{F}$. The matrix $\left[\boldsymbol{E}_1 \mid \boldsymbol{F}_2\right]$ has full rank, and the corresponding hybrid input-output representation is given by

$$\left[\begin{array}{c} e_1 \\ e_3 \\ e_4 \\ e_5 \\ \hdashline f_2 \end{array}\right] = -\underbrace{\left[\begin{array}{cccc:c} 0 & 0 & 0 & -r & -1 \\ 0 & 0 & 0 & -r & 0 \\ 0 & 0 & 0 & -1 & 0 \\ r & r & 1 & 0 & 0 \\ \hdashline 1 & 0 & 0 & 0 & 0 \end{array}\right]}_{\boldsymbol{J}} \left[\begin{array}{c} f_1 \\ f_3 \\ f_4 \\ f_5 \\ \hdashline e_2 \end{array}\right]. \tag{13}$$

It is clear that $\boldsymbol{J}$ is a skew-symmetric matrix.

3.2.3. Explicit effort/flow constraint representation [12], [28]

Suppose that the matrix $\boldsymbol{E}_1(\boldsymbol{x})$ is chosen such that $\operatorname{rank}\left(\boldsymbol{E}_1(\boldsymbol{x})\right) = \operatorname{rank}(\boldsymbol{E}(\boldsymbol{x}))$ (it means that the columns of $\boldsymbol{E}_2(\boldsymbol{x})$ are linear combinations of columns of $\boldsymbol{E}_1(\boldsymbol{x})$). Then the matrix $\left[\boldsymbol{E}_1(\boldsymbol{x}) \mid \boldsymbol{F}_2(\boldsymbol{x})\right]$ is invertible [6] and one finds that

$$\left[\boldsymbol{E}_1(\boldsymbol{x}) \mid \boldsymbol{F}_2(\boldsymbol{x})\right]^{-1} \boldsymbol{E}(\boldsymbol{x}) =: \left[\overline{\boldsymbol{E}}_1(\boldsymbol{x}) \mid \overline{\boldsymbol{E}}_2(\boldsymbol{x})\right] = \left[\begin{array}{c:c} \boldsymbol{I}_{n_1} & -\boldsymbol{J}_{21}^{\mathrm{T}}(\boldsymbol{x}) \\ \hdashline 0 & \boldsymbol{J}_{22}(\boldsymbol{x}) \end{array}\right].$$

Since the columns of $\boldsymbol{E}_2(\boldsymbol{x})$ are linear combinations of the columns of $\boldsymbol{E}_1(\boldsymbol{x})$, also the columns of $\bar{\boldsymbol{E}}_2(\boldsymbol{x})$ are linear combinations of the columns of $\bar{\boldsymbol{E}}_1(\boldsymbol{x})$. Therefore, $\boldsymbol{J}_{22}(\boldsymbol{x}) = 0$, and the Dirac structure is thus represented by

$$\mathcal{D}(\boldsymbol{x}) = \left\{(\boldsymbol{f},\boldsymbol{e}) \in T_z\mathcal{Z} \times T_z^*\mathcal{Z} : \boldsymbol{e} = -\tilde{\boldsymbol{J}}(\boldsymbol{x})\boldsymbol{f} + \boldsymbol{P}(\boldsymbol{x})\boldsymbol{\lambda},\ \boldsymbol{P}^{\mathrm{T}}(\boldsymbol{x})\boldsymbol{f} = 0\right\},$$

where

$$\tilde{\boldsymbol{J}}(\boldsymbol{x}) = \left[\begin{array}{c:c} \boldsymbol{J}_{11}(\boldsymbol{x}) & 0 \\ \hdashline 0 & 0 \end{array}\right],\ \boldsymbol{P}(\boldsymbol{x}) = \left[\begin{array}{c} -\boldsymbol{J}_{21}^{\mathrm{T}}(\boldsymbol{x}) \\ \hdashline \boldsymbol{I}_{n_2} \end{array}\right] \text{ and } \lambda \in \mathcal{R}^{n_2}.$$

This representation is called the explicit effort flow constraint representation. Note that $\mathrm{Im}(\boldsymbol{P}(\boldsymbol{x})) = \mathcal{P}_0(\boldsymbol{x})$.

Example 3 (*Continuation of Example 1*)

The rank of the matrix $\boldsymbol{E}$ is 4. We can choose $\boldsymbol{E}_1$ as in Example 2. Therefore the corresponding matrices $\tilde{\boldsymbol{J}}$ and $\boldsymbol{P}$ are given by

$$\tilde{\boldsymbol{J}} = \left[\begin{array}{cccc:c} 0 & 0 & 0 & -r & 0 \\ 0 & 0 & 0 & -r & 0 \\ 0 & 0 & 0 & -1 & 0 \\ r & r & 1 & 0 & 0 \\ \hdashline 0 & 0 & 0 & 0 & 0 \end{array}\right],\ \boldsymbol{P} = \left[\begin{array}{c} 1 \\ 0 \\ 0 \\ 0 \\ \hdashline 1 \end{array}\right].$$

3.2.4. Explicit flow/effort constraint representation [12], [28]

Suppose that $\boldsymbol{F}_2(\boldsymbol{x})$ is chosen such that $\mathrm{rank}\left(\boldsymbol{F}_2(\boldsymbol{x})\right) = \mathrm{rank}(\boldsymbol{F}(\boldsymbol{x}))$. Note that also $\left[\boldsymbol{E}_1(\boldsymbol{x}) \;\vdots\; \boldsymbol{F}_2(\boldsymbol{x})\right]$ is an invertible matrix. Similarly as above it follows that $\boldsymbol{J}_{11}(\boldsymbol{x}) = 0$ and that the Dirac structure is represented by

$$\mathcal{D}(\boldsymbol{x}) = \left\{(\boldsymbol{f},\boldsymbol{e}) \in T_z\mathcal{Z} \times T_z^*\mathcal{Z} : \boldsymbol{f} = -\tilde{\boldsymbol{J}}(\boldsymbol{x})\boldsymbol{e} + \boldsymbol{G}(\boldsymbol{x})\boldsymbol{\lambda}, \boldsymbol{G}^{\mathrm{T}}(\boldsymbol{x})\boldsymbol{e} = 0\right\},$$

where

$$\tilde{\boldsymbol{J}}(\boldsymbol{x}) = \left[\begin{array}{c:c} 0 & 0 \\ \hdashline 0 & \boldsymbol{J}_{22}(\boldsymbol{x}) \end{array}\right],\ \boldsymbol{G}(\boldsymbol{x}) = \left[\begin{array}{c} \boldsymbol{I}_{n_1} \\ \hdashline \boldsymbol{J}_{21}(\boldsymbol{x}) \end{array}\right] \text{ and } \lambda \in \mathcal{R}^{n_1}.$$

This representation is called the explicit flow effort constraint representation. Note that $\mathrm{Im}(\boldsymbol{G}(\boldsymbol{x})) = \mathcal{G}_0(\boldsymbol{x})$.

Example 4 (*Continuation of Example 1*)

The rank of the matrix $\boldsymbol{F}$ is 3. Let $\boldsymbol{F}_2$ contain the 2$^{\text{nd}}$, 4$^{\text{th}}$, 5$^{\text{th}}$ columns of $\boldsymbol{F}$. Then the matrix $\boldsymbol{E}_1$ contains the 1$^{\text{st}}$, 3$^{\text{rd}}$ columns. The hybrid input-output Dirac structure is given by (10) and the matrix $\boldsymbol{J}$ is given by

$$\begin{bmatrix} e_1 \\ e_3 \\ \hdashline f_2 \\ f_4 \\ f_5 \end{bmatrix} = -\underbrace{\left[\begin{array}{cc:ccc} 0 & 0 & -1 & -r & 0 \\ 0 & 0 & 0 & -r & 0 \\ \hdashline 1 & 0 & 0 & 0 & 0 \\ r & r & 0 & 0 & 1 \\ 0 & 0 & 0 & -1 & 0 \end{array}\right]}_{\boldsymbol{J}} \begin{bmatrix} f_1 \\ f_3 \\ \hdashline e_2 \\ e_4 \\ e_5 \end{bmatrix}. \tag{14}$$

Therefore the corresponding matrices $\tilde{\boldsymbol{J}}$ and $\boldsymbol{G}$ are given by

$$\tilde{\boldsymbol{J}} = \left[\begin{array}{cc:ccc} 0 & 0 & 0 & 0 & 0 \\ 0 & 0 & 0 & 0 & 0 \\ \hdashline 0 & 0 & 0 & 0 & 0 \\ 0 & 0 & 0 & 0 & 1 \\ 0 & 0 & 0 & -1 & 0 \end{array}\right], \boldsymbol{G} = \left[\begin{array}{cc} 1 & 0 \\ 0 & 1 \\ \hdashline -1 & 0 \\ -r & -r \\ 0 & 0 \end{array}\right].$$

3.3. Equivalence between Dirac structures

Let us consider two Dirac structures represented in kernel form as

$$\mathcal{D}_{\mathrm{I}}(\boldsymbol{x}) = \left\{(\boldsymbol{f},\boldsymbol{e}) \in T_{\boldsymbol{z}}\mathcal{Z} \oplus T_{\boldsymbol{z}}^{*}\mathcal{Z} : \boldsymbol{F}_{\mathrm{I}}(\boldsymbol{x})\boldsymbol{f} + \boldsymbol{E}_{\mathrm{I}}(\boldsymbol{x})\boldsymbol{e} = 0\right\},$$
$$\mathcal{D}_{\mathrm{II}}(\boldsymbol{x}) = \left\{(\boldsymbol{f},\boldsymbol{e}) \in T_{\boldsymbol{z}}\mathcal{Z} \oplus T_{\boldsymbol{z}}^{*}\mathcal{Z} : \boldsymbol{F}_{\mathrm{II}}(\boldsymbol{x})\boldsymbol{f} + \boldsymbol{E}_{\mathrm{II}}(\boldsymbol{x})\boldsymbol{e} = 0\right\}.$$

Here, the matrices $\boldsymbol{F}_{\mathrm{I}}$, $\boldsymbol{E}_{\mathrm{I}}$, respectively, $\boldsymbol{F}_{\mathrm{II}}$, $\boldsymbol{E}_{\mathrm{II}}$ satisfy the conditions (6), (7).

Definition 10: (*Equivalence between Dirac structures*)

Dirac structures $\mathcal{D}_{\mathrm{I}}$, $\mathcal{D}_{\mathrm{II}}$ are equivalent on the set $\mathcal{S} \subseteq \mathcal{X}$, denoted as $\mathcal{D}_{\mathrm{I}} \underset{\mathcal{S}}{\sim} \mathcal{D}_{\mathrm{II}}$, if there is a n-dimensional matrix $\boldsymbol{K}(\boldsymbol{x})$ regular on $\mathcal{S}$ and a $2n$-dimensional permutation matrix $\boldsymbol{Q}$ of the form

$$\boldsymbol{Q} = \left[\begin{array}{c:c} \boldsymbol{Q}_o & \boldsymbol{Q}_d \\ \hdashline \boldsymbol{Q}_d & \boldsymbol{Q}_o \end{array}\right] = \underbrace{\left[\begin{array}{c:c} \boldsymbol{Q}_o & 0_{n\times n} \\ \hdashline 0_{n\times n} & \boldsymbol{Q}_o \end{array}\right]}_{\boldsymbol{Q}_{\mathrm{or}}} + \underbrace{\left[\begin{array}{c:c} 0_{n\times n} & \boldsymbol{Q}_d \\ \hdashline \boldsymbol{Q}_d & 0_{n\times n} \end{array}\right]}_{\boldsymbol{Q}_{\mathrm{pd}}},$$

such that

$$\boldsymbol{K}(\boldsymbol{x})\left[\boldsymbol{F}_{\mathrm{I}}(\boldsymbol{x}) \,\vdots\, \boldsymbol{E}_{\mathrm{I}}(\boldsymbol{x})\right] = \left[\boldsymbol{F}_{\mathrm{II}}(\boldsymbol{x}) \,\vdots\, \boldsymbol{E}_{\mathrm{II}}(\boldsymbol{x})\right]\boldsymbol{Q},\ \forall \boldsymbol{x} \in \mathcal{S}. \tag{15}$$

Remark 2 (*Equivalence between Dirac structures*)

The first matrix $\boldsymbol{Q}_{\mathrm{or}}$ represents the ordering of power variables and the second one $\boldsymbol{Q}_{\mathrm{pd}}$ represents the impact of partial dualization procedure.

Example 5 (*Continuation of Example 2 and Example 4*)

Consider Dirac structures $\mathcal{D}_{\mathrm{I}}$, $\mathcal{D}_{\mathrm{II}}$ described by (13) respectively (14). They are equivalent on $\mathcal{R}^5$ since we can find the matrices $\boldsymbol{K}, \boldsymbol{Q}$

$$\boldsymbol{K}=\begin{bmatrix}1&0&0&0&-r\\0&1&0&0&-r\\0&0&0&0&-1\\0&0&0&1&0\\0&0&1&0&0\end{bmatrix},\ \boldsymbol{Q}_o=\begin{bmatrix}1&0&0&0&0\\0&1&0&0&0\\0&0&0&1&0\\0&0&0&0&1\\0&0&1&0&0\end{bmatrix},\boldsymbol{Q}_d=0.$$

such that (15) is satisfied. Since $\boldsymbol{Q}_d=0$, $\mathcal{D}_{\mathrm{I}}=\mathcal{D}_{\mathrm{II}}$ on $\mathcal{R}^5$.

3.4. Composition of Dirac structures

In this subsection we investigate the compositionality properties of Dirac structures. Physically it seems clear that the composition of a number of power-conserving interconnections with partially shared power variables yields again a power-conserving interconnection. In [28] is shown how this can be formalized within the framework of Dirac structures.

Consider Dirac structures $\mathcal{D}_1\subset T\mathcal{Z}_1\oplus\mathcal{V}_s\oplus T^*\mathcal{Z}_1\oplus\mathcal{V}_s^*$, $\mathcal{D}_2\subset T\mathcal{Z}_2\oplus\mathcal{V}_s\oplus T^*\mathcal{Z}_2\oplus\mathcal{V}_s^*$ with respect to the following bilinear form

$$\begin{gathered}\ll\left(\boldsymbol{f}_1^a,\boldsymbol{f}_s^a,\boldsymbol{e}_1^a,\boldsymbol{e}_s^a\right),\left(\boldsymbol{f}_1^b,\boldsymbol{f}_s^b,\boldsymbol{e}_1^b,\boldsymbol{e}_s^b\right)\gg_1:=\\ \left\langle\boldsymbol{e}_1^a\mid\boldsymbol{f}_1^b\right\rangle+\left\langle\boldsymbol{e}_1^b\mid\boldsymbol{f}_1^a\right\rangle+\left\langle\boldsymbol{e}_s^a\mid\boldsymbol{f}_s^b\right\rangle+\left\langle\boldsymbol{e}_s^b\mid\boldsymbol{f}_s^a\right\rangle,\\ \ll\left(\boldsymbol{f}_2^a,\boldsymbol{f}_s^a,\boldsymbol{e}_2^a,\boldsymbol{e}_s^a\right),\left(\boldsymbol{f}_2^b,\boldsymbol{f}_s^b,\boldsymbol{e}_2^b,\boldsymbol{e}_s^b\right)\gg_2:=\\ \left\langle\boldsymbol{e}_2^a\mid\boldsymbol{f}_2^b\right\rangle+\left\langle\boldsymbol{e}_2^b\mid\boldsymbol{f}_2^a\right\rangle-\left\langle\boldsymbol{e}_s^a\mid\boldsymbol{f}_s^b\right\rangle-\left\langle\boldsymbol{e}_s^b\mid\boldsymbol{f}_s^a\right\rangle.\end{gathered}$$

Here $\boldsymbol{f}_i$, $i=1,2$, represent the flow variables corresponding to $T\mathcal{Z}_i$. Similarly, $\boldsymbol{e}_i$, $i=1,2$, represent the effort variables corresponding to $T^*\mathcal{Z}_i$. Also, $\boldsymbol{f}_s$, $\boldsymbol{e}_s$ represent the shared power variables corresponding to $\mathcal{V}_s$, respectively to $\mathcal{V}_s^*$. The power variables $\boldsymbol{f}_s$, $\boldsymbol{e}_s$ are outgoing variables for $\mathcal{D}$ and incoming variables for $\mathcal{D}_2$. (Of course this is not the most general situation (some of the shared variables of $\mathcal{D}_2$ can be also outgoing. However, the generality is not lost and the results are more transparent in this case.) Let us now define, based on $\mathcal{D}_1$ and $\mathcal{D}_2$, the space

$$\begin{aligned}\mathcal{D}_{12}:=\Big\{&\left(\boldsymbol{f}_1,\boldsymbol{f}_2,\boldsymbol{e}_1,\boldsymbol{e}_2\right)\in T\mathcal{Z}_1\oplus T\mathcal{Z}_2\oplus T^*\mathcal{Z}_1\oplus T^*\mathcal{Z}_2:\\ &\exists\left(\boldsymbol{f}_s,\boldsymbol{e}_s\right)\in\mathcal{V}_s\oplus\mathcal{V}_s^*\ \text{s.t.}\left(\boldsymbol{f}_1,\boldsymbol{f}_s,\boldsymbol{e}_1,\boldsymbol{e}_s\right)\in\mathcal{D}_1\,\text{and}\left(\boldsymbol{f}_2,\boldsymbol{f}_s,\boldsymbol{e}_2,\boldsymbol{e}_s\right)\in\mathcal{D}_2\Big\}.\end{aligned}\tag{16}$$

Theorem 1 [28] (*Composition of two Dirac structures*)

Let $\mathcal{D}_1$, $\mathcal{D}$ be Dirac structures with respect to $\ll,\gg_1$, respectively $\ll,\gg_2$. Then $\mathcal{D}_{12}$ defined in (16) *is a Dirac structure with respect to the bilinear form $\ll,\gg_{1,2}$ defined on $T\mathcal{Z}_1\oplus T\mathcal{Z}_2\oplus T^*\mathcal{Z}_1\oplus T^*\mathcal{Z}_2$ as*

$$\ll \left(\boldsymbol{f}_1^a, \boldsymbol{f}_2^a, \boldsymbol{e}_1^a, \boldsymbol{e}_2^a\right), \left(\boldsymbol{f}_1^b, \boldsymbol{f}_2^b, \boldsymbol{e}_1^b, \boldsymbol{e}_2^b\right) \gg_1 := \left\langle \boldsymbol{e}_1^a \mid \boldsymbol{f}_1^b \right\rangle + \left\langle \boldsymbol{e}_1^b \mid \boldsymbol{f}_1^a \right\rangle + \left\langle \boldsymbol{e}_2^a \mid \boldsymbol{f}_2^b \right\rangle + \left\langle \boldsymbol{e}_2^b \mid \boldsymbol{f}_2^a \right\rangle .$$

Remark 3 (*Composition of two Dirac structures*) One can see that the dimension of the composed Dirac structure is $\dim\left(\mathcal{Z}_1\right) + \dim\left(\mathcal{Z}_2\right)$. This theorem represents the mathematical formulation of the tearing concept for the power conserving interconnections.

4. Geometric formulation of generalized junction structures

The main result of this paper is contained in this section. We prove that a generalized junction structure can be formulated as a Dirac structure. The proof of this statement is given in section 4.1. How one can practically determine the Dirac structure from the generalized junction structure is detailed in section 4.2.

4.1. Generalized junction structure is Dirac structure

In this subsection we prove that a generalized junction structure can be related to a Dirac structure. Hereafter, for the simplicity of presentation, the linear spaces $\mathcal{V}, \mathcal{V}^*$ are identified with $\mathcal{R}^m$, $m \in \mathcal{N}$, and the duality product is identified with the Euclidian inner product, i.e., $\left\langle \boldsymbol{e} \mid \boldsymbol{f} \right\rangle = \boldsymbol{e}^{\mathrm{T}} \boldsymbol{f}$.

Theorem 2 (*Generalized junction structure defines a Dirac structure*)
Consider a generalized junction structure that contains n ports and whose flows belong to $T_{\boldsymbol{x}}\mathcal{X} \times \mathcal{V}$ and whose efforts belong to $T_{\boldsymbol{x}}^*\mathcal{X} \times \mathcal{V}^*$. Here, $\mathcal{X}$ is a differentiable manifold and the flows of $\pi \in \Pi^{\mathrm{R}} \cup \Pi^{\mathrm{Se}} \cup \Pi^{\mathrm{Sf}}$ belong to the space $\mathcal{V}$. The generalized junction structure can be related to a Dirac structure defined on the space $\mathcal{X} \times \mathcal{V}$.

Proof: The proof is based on Theorem 1. Firstly, we prove that 1-junctions, 0-junctions, two-port transformers and two-port gyrators can be related to Dirac structures. Let us consider an 1-junction. Its constitutive relation is given by

$$-\sum_{i=1}^{k} e_i + \sum_{i=k+1}^{l} e_i = 0, \tag{17}$$

$$f_1 = f_2 = \dots = f_l . \tag{18}$$

Here, f_i, e_i, $i = \overline{1,k}$ are the power variables of the incoming ports and f_i, e_i, $i = \overline{k+1,l}$ are the power variables of the outgoing ports. Multiplying (17) by f_1 and using (18) it follows that

$$-\sum_{i=1}^{k} f_i e_i + \sum_{i=k+1}^{l} f_i e_i = P_{\text{out}} - P_{\text{in}} = 0 .$$

In other words the 1-junction is a power conserving interconnection. To prove that the 1-junction can be related to a Dirac structure we also have to prove that its set of admissible flows and efforts is l dimensional. Indeed, if we fix f_1 and e_i, $i=\overline{2,l}$ then the other flows (f_i, $i=\overline{2,l}$) and the effort e_1 are uniquely determined. Therefore, the dimension of the set of admissible flows and efforts is l. A similar result can be proved for a 0-junction.

Let us consider now a two-port transformer. Its constitutive relation can be described by

$$\underbrace{\begin{bmatrix} 0 \\ -r(\boldsymbol{x}) \end{bmatrix}}_{\boldsymbol{F}_{\text{in}}(\boldsymbol{x})} f_1 + \underbrace{\begin{bmatrix} 0 \\ 1 \end{bmatrix}}_{\boldsymbol{F}_{\text{out}}(\boldsymbol{x})} f_2 + \underbrace{\begin{bmatrix} 1 \\ 0 \end{bmatrix}}_{\boldsymbol{E}_{\text{in}}(\boldsymbol{x})} e_1 + \underbrace{\begin{bmatrix} -r(\boldsymbol{x}) \\ 0 \end{bmatrix}}_{\boldsymbol{E}_{\text{out}}(\boldsymbol{x})} e_2 = 0 .$$

Here, $r(\boldsymbol{x})$ represents the ratio of the transformer. A straightforward computation shows that the conditions (8), (9) are fulfilled. Therefore, a Dirac structure can be related to the two-port transformer. A similar result holds for a two-port gyrator.

Secondly, a generalized junction structure is composed from the junctions and the transducers. If any of transducers has three or more ports then it can be decomposed into two-port transducers and junctions as shown in ([9], pp.74, 75 and 88). Therefore, a generalized junction structure can be seen as the composition of junctions and two-port transducers. Since all of them can be related to Dirac structures, their composition (see Theorem 1) is again a Dirac structure defined on $\mathcal{X}\times\mathcal{V}$. ■

Remark 4 (*A generalized junction structure defines a Dirac structure*) This theorem shows two things. The first one is that a generalized junction structure is a power conserving interconnection. It means that the power balance at its ports is zero. This property easily follows by writing down the power balances for every junction and transducer, and by summing all of them. The second is that its n power variables can be expressed as a linear function of the other n power variables.

4.2. Procedure for deriving Dirac structure from generalized junction structure

In this section we give an alternative proof of Theorem 2. This proof is constructive and leads to a procedure for practical deriving the Dirac structure from a generalized junction structure. Before we give the procedure, some auxiliary results are derived. In section 4.2.1, the **I**nput-**O**utput **G**eneralized **J**unction **S**tructure (IOGJS) is defined. Some properties of an IOGJS are given in the section 4.2.2. In section 4.2.3

an algorithm for changing the incidence relations between ports and junctions of an IOGJS is given. How to transform a GJS into an IOGJS is shown in section 4.2.4. The constructive proof of Theorem 2 is given in section 4.2.5. Finally, section 4.2.6 deals with singular generalized junction structures.

4.2.1. Input-output generalized junction structure

Let us consider a Dirac structure represented by a hybrid input-output form (10). The equations relating the vectors $\boldsymbol{f}_1, \boldsymbol{f}_2, \boldsymbol{e}_1, \boldsymbol{e}_2$ are given by

$$\boldsymbol{e}_1 = -\boldsymbol{J}_{11}(\boldsymbol{x})\boldsymbol{f}_1 - \boldsymbol{J}_{21}^{\mathrm{T}}(\boldsymbol{x})\boldsymbol{e}_2, \tag{19}$$

$$\boldsymbol{f}_2 = \boldsymbol{J}_{21}(\boldsymbol{x})\boldsymbol{f}_1 - \boldsymbol{J}_{22}(\boldsymbol{x})\boldsymbol{e}_2. \tag{20}$$

A bond graph representation of (19), (20) is given in Figure 6.

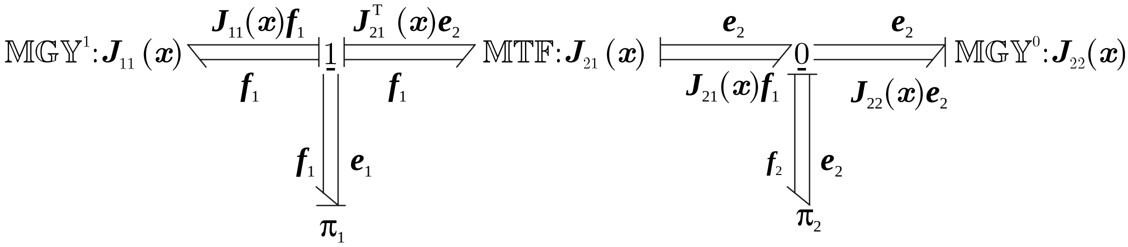

Figure 6: Bond graph representation of (19), (20).

$\mathbb{GY}^1\!:\boldsymbol{J}$ ($\mathbb{GY}^0\!:\boldsymbol{J}$) means that the constitutive relation for the gyrator is given by $\boldsymbol{e} = \boldsymbol{J}\boldsymbol{f}$ (respectively, $\boldsymbol{f} = \boldsymbol{J}\boldsymbol{e}$). The graphical representation of (19), (20) is a generalized junction structure. It has a specific structure called input-output generalized junction structure (IOGJS), and is denoted by $\mathbb{IOGJS}$. The formal definition of an IOGJS is given below.

Definition 11 (*Definition of IOGJS*)

A generalized junction structure is an IOGJS if the following conditions are satisfied:

[D5a] *The number of ports joining a junction is always one.*

[D5b] *The vertices of a TF-link are always different types of junctions, that is, a either* 1*-junction and a* 0*-junction or a* 0*-junction and a* 1*-junction.*

[D5c] *The vertices of a GY-link are always the same type of junctions, that is, either* 1*-junctions or* 0*-junctions.*

This definition leads to the definition of an **I**nput-**O**utput **G**eneralized **B**ond **G**raph (IOGBG).

Definition 12 (*Definition of IOGBG*)

A generalized bond graph is an IOGBG if its generalized junction structure is an IOGJS.

Due to specific form of IOGJS, its causal assignment is straightforward. If a port joins a 1-junction then it has effort out causality. If a port joins a 0-junction then it has flow out causality. These two rules together with standard rules for junctions, and two-port transducers, (see [13], pp. 36) uniquely define the causality of an IOGJS. If the output and input variables are chosen in accordance with the previously defined causality assignment then the input-output relations can be straightforwardly obtained as shown in Algorithm 1.

Before we present Algorithm 1 the incidence function σ_β is defined. Assume that a bond β joins a node $\eta \in \mathrm{E} \cup \Xi \cup \mathrm{T}$, then as before

$$\sigma_\beta(\beta, \eta) = \begin{cases} 1, \text{if } \beta \text{ is outgoing in } \eta \\ -1, \text{if } \beta \text{ is incoming in } \eta \end{cases}.$$

Also, the bond β corresponding to two adjacent nodes $\eta_1, \eta_2 \in \mathrm{E} \cup \Xi \cup \mathrm{T}$ will be denoted by $\beta = \{\eta_1, \eta_2\}$.

Algorithm 1 (*Determination of $\boldsymbol{J}(\boldsymbol{x})$ from IOGJS*)

Goal: *Determining $\boldsymbol{J}(\boldsymbol{x})$, as well as n_1, n_2.*

Input: *An IOGJS denoted by $\mathbb{IOGJS}$.*

Step 1 (*Determination of n_1, n_2*) The integer n_1 is equal to the number of 1-junctions. The integer n_2 is equal to number of 0-junctions. 1-junctions are denoted by χ_j^1, $j = \overline{1, n_1}$ and 0-junctions are denoted by χ_i^0, $i = \overline{1, n_2}$.

Step 2 (*Determination the elements of $\boldsymbol{J}_2(\boldsymbol{x})$*)

The i, j^{th} element of $\boldsymbol{J}_2(\boldsymbol{x})$, $j_{i,j}^{12}(\boldsymbol{x})$, can be determined as shown in Table 2. Here $r(\boldsymbol{x})$ is the ratio of the transformer τ^{TF}.

Table 2

There is a P-link (χ_j^1, χ_i^0)	There is a TF-link $(\chi_j^1, \tau^{\mathrm{TF}}, \chi_i^0)$	$j_{i\,j}^{1}(\boldsymbol{x})$
No	No	0
Yes	No	$j_{i,j}^{12}(\boldsymbol{x}) = \sigma_\beta\left(\left\{\chi_j^1, \chi_i^0\right\}, \chi_j^1\right)$
No	Yes	$j_{i,j}^{12}(\boldsymbol{x}) = \dfrac{\sigma_\beta\left(\left\{\chi_j^1, \tau^{\mathrm{TF}}\right\}, \chi_j^1\right)}{(r(\boldsymbol{x}))^{-\sigma_\beta\left(\left\{\chi_j^1, \tau^{\mathrm{TF}}\right\}, \chi_j^1\right)}}$

Step 2 (*Determination the elements of $\boldsymbol{J}_{11}(\boldsymbol{x})$*)

The (i, j^{th}) element $(i < j)$ of $\boldsymbol{J}_{11}(\boldsymbol{x})$, $j_{i,j}^{11}(\boldsymbol{x})$, can be determined as shown in Table 3. Here $r(\boldsymbol{x})$ is the ratio of the gyrator τ^{GY}.

Table 3

There is a GY-link $\left(\chi_i^1, \tau^{\mathrm{GY}}, \chi_j^1\right)$.	$j_{i,j}^{11}(\boldsymbol{x}) = -j_{j,i}^{11}(\boldsymbol{x})$, $(i < j)$
No	0
Yes	$j_{i,j}^{11}(\boldsymbol{x}) = r(\boldsymbol{x}) \cdot \sigma_\beta\left(\left\{\chi_i^1, \tau^{\mathrm{GY}}\right\}, \chi_i^1\right)$

Step 3 (*Determination the elements of* $\boldsymbol{J}_{22}(\boldsymbol{x})$)

The $\left(i, j^{\mathrm{th}}\right)$ element $(i < j)$ of $\boldsymbol{J}_{22}(\boldsymbol{x})$, $j_{i,j}^{22}(\boldsymbol{x})$, can be determined as shown in Table 4. Here $r(\boldsymbol{x})$ is the ratio of the gyrator τ^{GY}.

Table 4

There is a GY-link $\left(\chi_i^0, \tau^{\mathrm{GY}}, \chi_j^0\right)$.	$j_{i,j}^{22}(\boldsymbol{x}) = -j_{j,i}^{22}(\boldsymbol{x})$, $(i<j)$
No	0
Yes	$j_{i,j}^{22}(\boldsymbol{x}) = r(\boldsymbol{x}) \cdot \sigma_\beta\left(\left\{\chi_i^0, \tau^{\mathrm{GY}}\right\}, \chi_i^0\right)$

4.2.2. Some properties of IOGJS

In section 3.3 an equivalence relation between Dirac structures has been introduced. This will be used to define an equivalence relation between IOGJS's.

Definition 13 (*Equivalence between IOGJS's*)

Consider two input-output generalized junction structures, $\mathbb{IOGJS}_{\mathrm{I}}$, $\mathbb{IOGJS}_{\mathrm{II}}$. *Their corresponding Dirac structures are represented in hybrid input-output form and denoted by* $\mathcal{D}_{\mathrm{I}}$ *and* $\mathcal{D}_{\mathrm{II}}$. *The generalized junction structures* $\mathbb{IOGJS}_{\mathrm{I}}$, $\mathbb{IOGJS}_{\mathrm{II}}$ *are equivalent on* $\mathcal{S}$, $\mathbb{IOGJS}_{\mathrm{I}} \underset{\mathcal{S}}{\sim} \mathbb{IOGJS}_{\mathrm{II}}$, *if and only if* $\mathcal{D}_{\mathrm{I}} \underset{\mathcal{S}}{\sim} \mathcal{D}_{\mathrm{II}}$.

The transformations that convert an IOGJS into an equivalent IOGJS are called equivalence transformations. Here, we consider three types of equivalence transformations. The first one, the partial dualization procedure applied to a port (see Figure 4), is denoted by $\boldsymbol{T}_{\pi_i}^0$.

Theorem 3 (*Partial dualization procedure applied to a port*)

Consider an IOGJS, denoted by $\mathbb{IOGJS}$. *Suppose that the partial dualization procedure is applied to port* π_i. *The obtained generalized junction structure is again an equivalent IOGJS, denoted by* $\mathbb{IOGJS}_{\mathrm{eq}}$.

Proof: The proof of Theorem 3 is given in Appendix 1.

The second one is called a reconnecting procedure via a transformer, and denoted by $\boldsymbol{T}_{\pi_i,\pi_j}^1$.

Theorem 4 (*Reconnecting procedure via a transformer*)

Consider an IOGJS, denoted by $\mathbb{IOGJS}$. *Suppose that there are two ports* π_i, π_{n_1+j} *joining 1-junction* χ_i^1, *0-junction* χ_j^0, *respectively. Suppose that there is either a P-link* $\left(\chi_i^1,\chi_j^0\right)$ *or a TF-link* $\left(\chi_i^1,\tau^{\mathrm{TF}},\chi_j^0\right)$, *see Figure 7a. In the latter case the ratio of* τ^{TF}, $r(\boldsymbol{x})$, *is assumed to be different from zero* $\forall \boldsymbol{x}\in\mathcal{S}$. *Then there exists an IOGJS, denoted by* $\mathbb{IOGJS}_{\mathrm{eq}}$, *such that* π_i, π_{n_1+j} *joins* χ_j^0, χ_i^1, *see Figure 7b, and* $\mathbb{IOGJS}\underset{\mathcal{S}}{\sim}\mathbb{IOGJS}_{\mathrm{eq}}$.

Proof: The proof of Theorem 4 is given in Appendix 1.

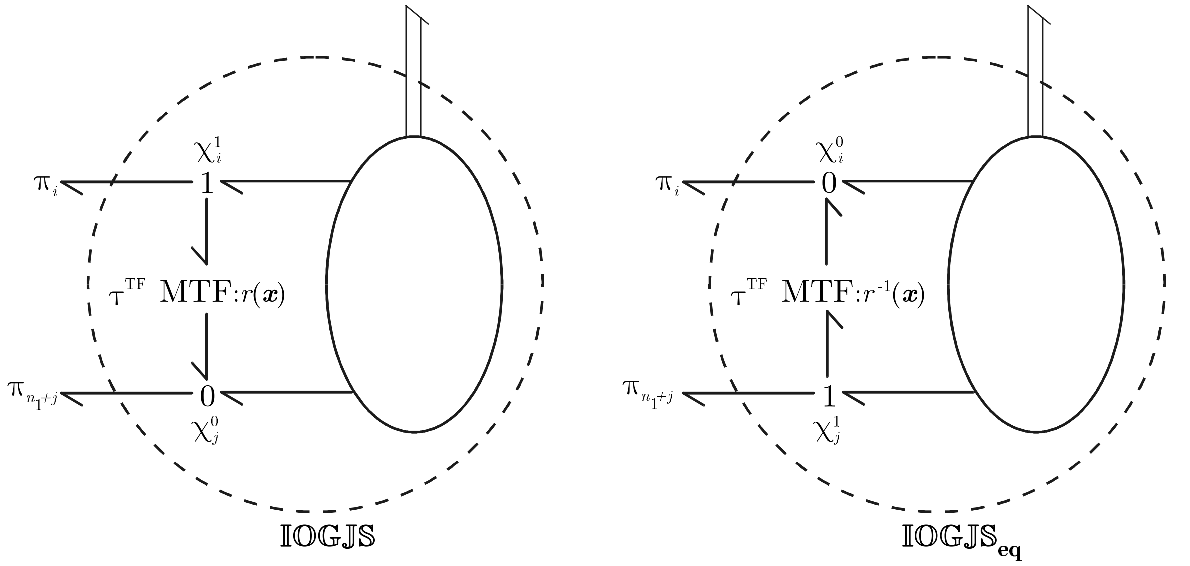

a) *b*)

Figure 7: Reconnecting procedure via transformer

The third equivalence transformation is called the reconnecting procedure via a gyrator and is denoted by $\boldsymbol{T}^2_{\pi_i,\pi_j}$.

Theorem 5 (*Reconnecting procedure via a gyrator*)

Consider an IOGJS, denoted by $\mathbb{IOGJS}$. *Suppose that there are two ports* π_i *and* π_j *joining* χ_i^p, χ_j^p, *respectively and* $p\in\{0,1\}$. *Suppose that there is a GY-link* $\left(\chi_i^p,\tau^{\mathrm{TF}},\chi_j^p\right)$, *see Figure 8a, and the ratio of* τ^{GY}, $r(\boldsymbol{x})$, *is different from zero* $\forall \boldsymbol{x}\in\mathcal{S}$. *Then there exists an IOGJS, denoted by* $\mathbb{IOGJS}_{\mathrm{eq}}$, *such that* π_i, π_j *are incident on the junctions belonging to the set* Ξ^{1-p}, *see Figure 8b, and* $\mathbb{IOGJS}\underset{\mathcal{S}}{\sim}\mathbb{IOGJS}_{\mathrm{eq}}$.

Proof: The proof of Theorem 5 is given in Appendix 1.

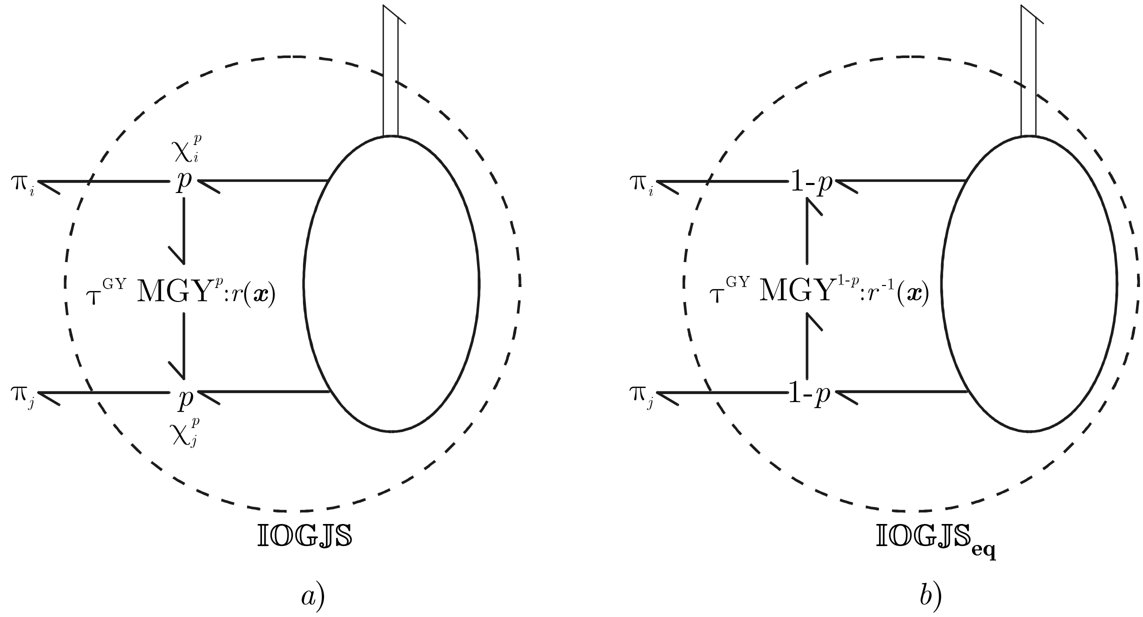

Figure 8: Reconnecting procedure via gyrator

4.2.3. Algorithm for changing of incidence relations between ports and junctions

It is clear from section 4.2.1 that the type of incidence relation between ports and junctions determine which of power variables are *computational* outputs and which of them are *computational* inputs with respect to the generalized junction structure. The computational outputs are the flows of the ports adjoining the 0-junctions and the efforts of the ports adjoining the 1-junctions. Consequently, the computational inputs are the efforts of the ports adjoining the 0-junctions and the flows of the ports adjoining the 1-junctions. On the other hand, which of the power variables is output and which of them is input should depend on the type of a port. For example, if a port $\pi \in \Pi^{Se}$ then its effort is an input and its flow is an output. Hence if π joins a 1-junction then its computational input is flow and its computational output is effort. Therefore we have a conflict. This conflict can be resolved by finding an equivalent IOGJS such that π and a 0-junction are incident.

Motivated by the previous discussion we present an algorithm for changing the incidence relations between ports and junctions. The set of ports is split as $\Pi = \Pi^{I} \cup \Pi^{II} \cup \Pi^{III}$. Suppose that a port π joins a junction χ. If π belongs to Π^{I} then the incidence relation between π and χ can not be changed. If π belongs to Π^{II} then the incidence relation between π and χ can be changed. Finally, if π belongs to Π^{III} then the incidence relations between π and χ may be changed as long as χ does not belong to Ξ^{p} ($p \in \{0,1\}$).

Algorithm 2 (*Changing the incidences between ports and junctions*)

Goal: *Find an equivalent IOGJS such that the number of the ports* $\pi \in \Pi^{\mathrm{III}}$ *adjoining the junctions belonging to the set* Ξ^p *is maximized.*

Input: $\mathbb{IOGJS}$*, the definition of the sets* Π^{I}*,* Π^{II}*,* Π^{III}*, and the number* p*.*

Remark: χ_a*,* π_a *are incident and* χ_b*,* π_b *are incident.*

Choose any port π_a belonging to the set Π^{III}.

IF $\chi_a \notin \Xi^p$ THEN

IF $\exists \pi_b \in \Pi^{\mathrm{II}}$ such that the following conditions are satisfied

$\chi_b \notin \Xi^p$

There is either a P-link (χ_a, χ_b) or TF-link $(\chi_a, \tau^{\mathrm{TF}}, \chi_b)$ THEN

$\mathbb{IOGJS} := T^1_{\pi_a,\pi_b}(\mathbb{IOGJS})$.

ELSE IF $\exists \pi_b \in \Pi^{\mathrm{II}}$ such that the following conditions are satisfied

$\chi_b \notin \Xi^p$

There is a GY-link $(\chi_a, \tau^{\mathrm{GY}}, \chi_b)$ THEN

$\mathbb{IOGJS} := T^2_{\pi_a,\pi_b}(\mathbb{IOGJS})$

ELSE IF $\exists \pi_b \in \Pi^{\mathrm{III}}$ such that the following conditions are satisfied

$\chi_b \notin \Xi^p$

There is a GY-link $(\chi_a, \tau^{\mathrm{GY}}, \chi_b)$ THEN

$\mathbb{IOGJS} := T^2_{\pi_a,\pi_b}(\mathbb{IOGJS})$

Repeat until all ports belonging to the set Π^{III} have been used.

Remark 5 (*Algorithm 2*)

Suppose that after applying Algorithm 2 to an IOGJS, some of the ports belonging to Π^{III} join junctions that do not belong to Ξ . Then the following can be concluded:

[A2a] There are no basic links between the junctions of these ports and other junctions joining the ports belonging to Π^{II}.

[A2b] There are no GY-links between the junctions adjoining these ports.

Hence, if $p = 0$ then the effort of $\pi \in \Pi^{\mathrm{III}}$ adjoining the 1-junction can be expressed as

$$e = \sum_{\pi_i \in \Pi^{\mathrm{III}} \setminus \{\pi\}} \alpha_i(\boldsymbol{x}) e_i + \sum_{\pi_i \in \Pi^{\mathrm{I}}} \beta_i(\boldsymbol{x}) (\text{either } e_i \text{ or } f_i).$$

Here, e is the effort of π, e_i, f_i are the power variables of π_i, and $\alpha_i(\boldsymbol{x}), \beta_i(\boldsymbol{x})$ are smooth scalar functions. A similar relation can be obtained for $p=1$, that is

$$f=\sum_{\pi_i\in\Pi^{\mathrm{III}}\setminus\{\pi\}}\alpha_i(\boldsymbol{x})f_i+\sum_{\pi_i\in\Pi^{\mathrm{I}}}\beta_i(\boldsymbol{x})(\text{either } e_i \text{ or } f_i).$$

where f is the flow of π.

4.2.4. Transformation of GJS into IOGJS

A generalized junction structure is not an IOGJS if at least one the conditions of Definition 11 is not satisfied. There are four cases in which the conditions of Definition 11 are violated.

Consider a part of GJS shown in Figure 9. Let the number of ports joining the junction χ^p be larger than one. Then condition [D5a] is not satisfied. This violation is called *violation of Type 1.*

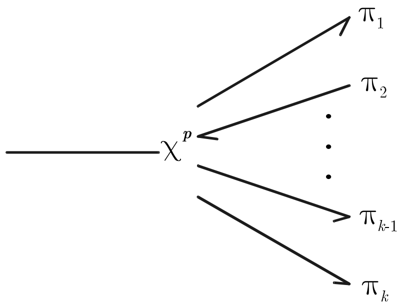

Figure 9: Violation of Type 1

This violation can be resolved as shown in Figure 10. All ports except one are replaced by the combination bond—junction—port. The orientation of the added bonds is the same as one of the replaced ports. If p=1 (p=0) then the added junctions belong to Ξ^0 (Ξ^1). The choice of the bond that is not replaced is arbitrary.

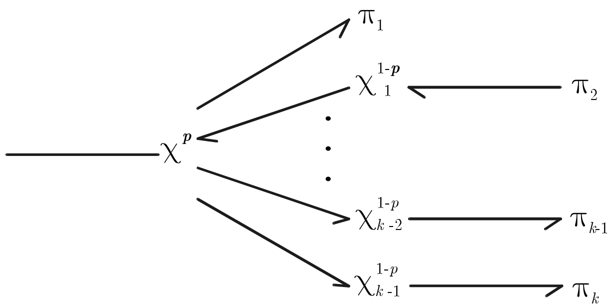

Figure 10: Solution for the violation of Type 1

Consider the part of a GJS shown in Figure 11. Let the number of ports incident on the junction χ^p be zero. Then, again condition [D5a] is not satisfied. This violation is called *violation of Type 2.*

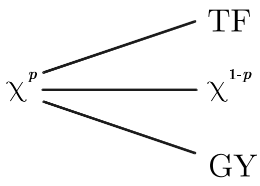

Figure 11: Violation of Type 2

The violation of Type 2 can be resolved as shown in Figure 12. If $p = 1$ then the zero effort source is connected to the junction χ^1. If $p = 0$ then the zero flow source is connected to the junction χ^0.

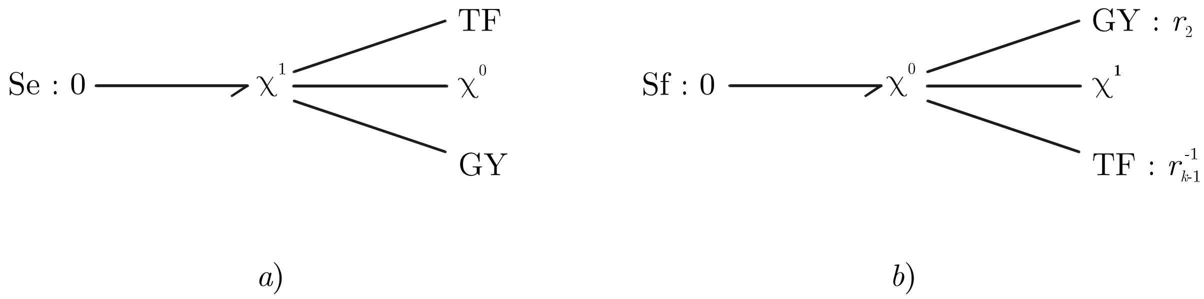

Figure 12: Solution for the violation of Type 2 ***a)*** ***p*=1** ***b)*** ***p*=0**

Consider the part of a GJS shown in Figure 13. Let there exist a TF-link whose vertices are junctions of the same type. Then the condition [D5b] is not satisfied. This violation is called *violation of Type 3*.

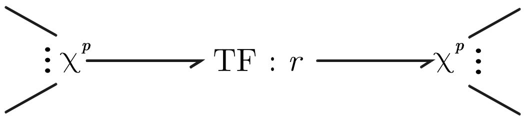

Figure 13: Violation of Type 3

It can be resolved as shown in Figure 14. If $p = 0$ then the entering bond of the transformer is replaced by a combination bond—1-junction—bond. To ensure that the first condition of Definition 11 is satisfied a zero effort source is connected to the added 1-junction. If $p = 1$ then the leaving bond of the transformer is replaced by a combination bond—0-junction—bond. To ensure that the first condition of Definition 11 is satisfied a zero flow source is connected to the added 0-junction.

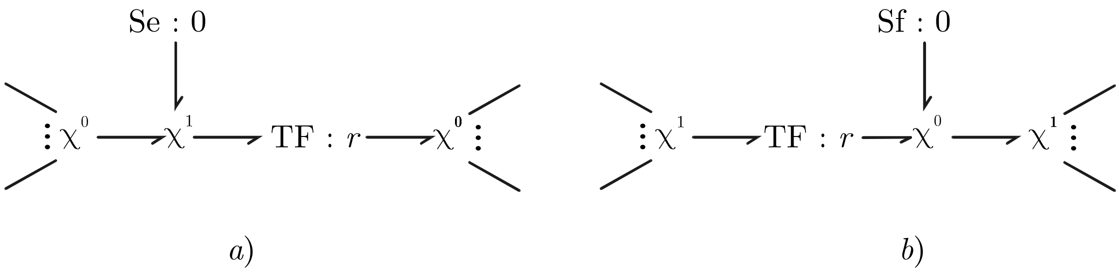

Figure 14: Solution for the violation of Type 3 ***a)*** ***p*=0** ***b)*** ***p*=1**

Consider the part of GJS shown in Figure 15. Let there exist a GY-link which vertices are the junctions of the different types. Therefore the condition [D5c] is not satisfied. This violation is called *violation of Type 4*.

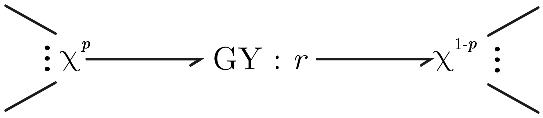

Figure 15: Violation of Type 4

It can be resolved as shown in Figure 16. If $p = 0$ then the entering bond of the gyrator is replaced by a combination bond—1-junction—bond, and a zero effort source is connected to the added 1-junction. If $p = 1$ then the leaving bond of transformer GY is replaced by a combination bond—1-junction—bond, and a zero effort source is connected to the added 1-junction.

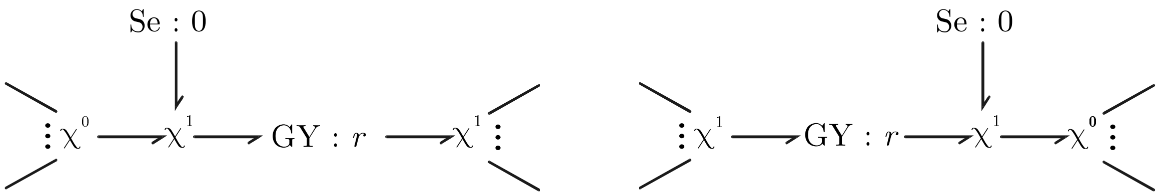

a) *b*)

Figure 16: Solution for the violation of Type 4 *a*) *p*=0 *b*) *p*=1

Therefore, the procedure for transforming an arbitrary GJS into an IOGJS is reduced to finding the parts of GJS that violate the conditions of Definition 11 and to resolving these violations as shown in Figure 10, Figure 12, Figure 14, Figure 16. In this way an IOGJS is obtained.

The dimension of the Dirac structure that corresponds to the obtained IOGJS is larger than the dimension of the one corresponding to the original GJS. The dimension is increased by the number of violations of the Type 2, Type 3 and Type 4. The obtained IOGJS is called an extended IOGJS. Also, the corresponding generalized bond graph with extended IOGJS is called an extended IOGBG.

We introduce two new sets of ports Π^{Se_0} and Π^{Sf_0}. Here, Π^{S_0} (Π^{Sf_0}) stands for the set of ports that represent the connections of the extended IOGJS to added zero effort sources (added zero flow sources). Therefore, the set of ports of the extended IOGJS is given by

$$\Pi^{\mathrm{ex}} = \Pi \cup \Pi^{\mathrm{Se}_0} \cup \Pi^{\mathrm{Sf}_0}.$$

Here, n_{ex} stands for the number of ports of extended IOGJS. Now, some definitions that will be used in sequel are given.

Definition 14 (*Auxiliary junction*)

Consider an extended IOGJS. If a junction adjoins an added zero source then it is called an auxiliary junction.

Definition 15 (*Auxiliary variables*)

The auxiliary variables are the efforts of the auxiliary 0-junctions and the flows of the auxiliary 1-junctions.

Example 6 (*Continuation of Example 1*)

onsider the electrical circuit shown in Figure $5a$. The GBG model of this system is shown in Figure $5b$. The GJS is not an IOGJS, since the ports π_1, π_2 adjoin the same 1-junction (violation of Type 1). Also the transformer is adjacent on two 0-junctions (violation of Type 3). Those problems can be solved as shown in Figure 10 and Figure 14. In this way an extended IOGBG shown in Figure 17 is obtained.

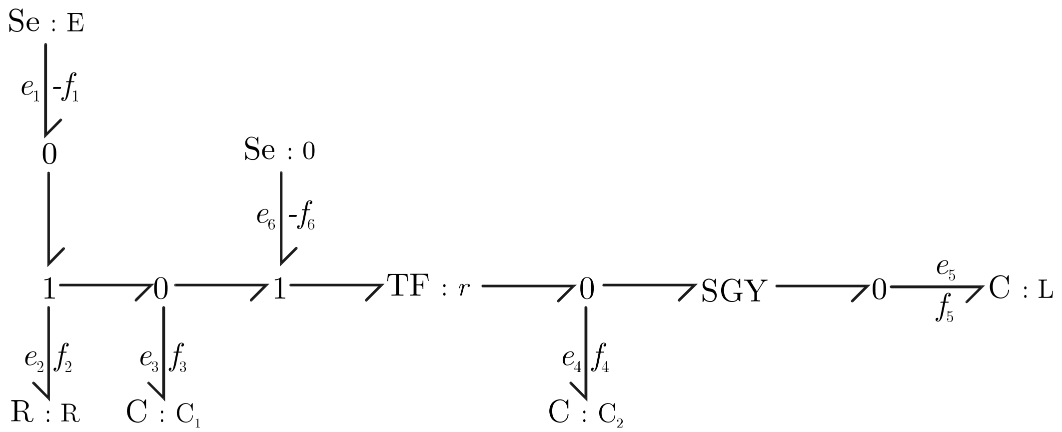

Figure 17: Extended IOGBG representation of electrical circuit shown in Figure 5*a*

4.2.5. Constructive proof of Theorem 2

In this section we give an alternative proof of Theorem 2. All necessary tools for this proof have been developed in subsections 4.2.1-4.2.4. The proof of Theorem 2 is constructive and it is given as an algorithm containing five steps.

Algorithm 3 (*Deriving the Dirac structure from GJS*)

Goal: *Deriving the Dirac structure from GJS*

Input: *GJS that satisfies the conditions [As1a]-[As1e]*

Step 1: Transform GJS into the extended IOGJS as shown in section 4.2.4.

Step 2: Apply Algorithm 1 to the extended IOGJS obtained in the step 1.

Step 3: Apply Algorithm 2 to the extended IOGJS obtained in the step 1 ($\Pi^{\mathrm{I}} = \varnothing$, $\Pi^{\mathrm{III}} = \Pi^{\mathrm{Se}_0}$, $\Pi^{\mathrm{II}} = \Pi^{\mathrm{ex}} \setminus \Pi^{\mathrm{Se}_0}$ and $p = 0$).

Step 4: Apply Algorithm 2 to the IOGJS obtained in the step 2 ($\Pi^{\mathrm{I}} = \Pi^{\mathrm{Se}_0}$, $\Pi^{\mathrm{III}} = \Pi^{\mathrm{Sf}_0}$, $\Pi^{\mathrm{II}} = \Pi$ and $p = 1$).

Step 5: Eliminate all added zero source ports, all auxiliary junctions and all basic links where one of the vertices is an auxiliary junction.

Consider a GJS satisfying the conditions [As1a]-[As1e]. After step 1 an extended IOGJS is obtained. The interconnection relations of the extended IOGJS are described by (step 2)

$$\begin{bmatrix} \boldsymbol{e}_1^{\mathrm{ex}} \\ \boldsymbol{f}_2^{\mathrm{ex}} \end{bmatrix} = -\boldsymbol{J}^{\mathrm{ex}}(\boldsymbol{x}) \begin{bmatrix} \boldsymbol{f}_1^{\mathrm{ex}} \\ \boldsymbol{e}_2^{\mathrm{ex}} \end{bmatrix}.$$

Here $\boldsymbol{f}_i^{\mathrm{ex}}, \boldsymbol{e}_i^{\mathrm{ex}}$, $i = 1,2$ are the power variables of the ports belonging to the set Π^{ex} and $\boldsymbol{J}^{\mathrm{ex}}(\boldsymbol{x})$ is a skew-symmetric matrix. Applying steps 3,4 to the IOGJS an equivalent extended IOGJS is obtained, whose interconnection relation can be expressed as

$$\begin{bmatrix} \boldsymbol{e}_1 \\ \boldsymbol{f}_2 \\ \hdashline \boldsymbol{e}_1^{\mathrm{Se}_0} \\ \boldsymbol{f}_2^{\mathrm{Se}_0} \\ \boldsymbol{e}_1^{\mathrm{Sf}_0} \\ \boldsymbol{f}_2^{\mathrm{Sf}_0} \end{bmatrix} = -\underbrace{\left[\begin{array}{c:ccccc} \boldsymbol{J}(\boldsymbol{x}) & 0 & \boldsymbol{J}_1^{\mathrm{T}}(\boldsymbol{x}) & \boldsymbol{J}_2^{\mathrm{T}}(\boldsymbol{x}) & 0 \\ \hdashline 0 & 0 & \boldsymbol{J}_3^{\mathrm{T}}(\boldsymbol{x}) & 0 & 0 \\ -\boldsymbol{J}_1(\boldsymbol{x}) & -\boldsymbol{J}_3(\boldsymbol{x}) & \boldsymbol{J}_4(\boldsymbol{x}) & \boldsymbol{J}_5^{\mathrm{T}}(\boldsymbol{x}) & \boldsymbol{J}_6^{\mathrm{T}}(\boldsymbol{x}) \\ -\boldsymbol{J}_2(\boldsymbol{x}) & 0 & -\boldsymbol{J}_7(\boldsymbol{x}) & \boldsymbol{J}_8(\boldsymbol{x}) & \boldsymbol{J}_9^{\mathrm{T}}(\boldsymbol{x}) \\ 0 & 0 & -\boldsymbol{J}_6(\boldsymbol{x}) & -\boldsymbol{J}_9(\boldsymbol{x}) & 0 \end{array}\right]}_{\boldsymbol{J}^{\mathrm{ex}}(\boldsymbol{x})} \begin{bmatrix} \boldsymbol{f}_1 \\ \boldsymbol{e}_2 \\ \hdashline \boldsymbol{f}_1^{\mathrm{Se}_0} \\ \boldsymbol{e}_2^{\mathrm{Se}_0} \\ \boldsymbol{f}_1^{\mathrm{Sf}_0} \\ \boldsymbol{e}_2^{\mathrm{Sf}_0} \end{bmatrix}.$$

Here, $\boldsymbol{e}_1, \boldsymbol{f}_1$ $(\boldsymbol{e}_2, \boldsymbol{f}_2)$ are the power variables of the ports belonging to Π and the adjoining 1-junctions (0-junctions), $\boldsymbol{e}_1^{\mathrm{Se}_0}, \boldsymbol{f}_1^{\mathrm{Se}_0}$ $(\boldsymbol{e}_2^{\mathrm{Se}_0}, \boldsymbol{f}_2^{\mathrm{Se}_0})$ are the power variables of the added zero effort sources adjoining the 1-junctions (0-junctions) and $\boldsymbol{e}_1^{\mathrm{Sf}_0}, \boldsymbol{f}_1^{\mathrm{Sf}_0}$ $(\boldsymbol{e}_2^{\mathrm{Sf}_0}, \boldsymbol{f}_2^{\mathrm{Sf}_0})$ are the power variables of the added zero flow sources adjoining the 1-junctions (0-junctions).

Given that Algorithm 2 is applied in step 3 there are only P-links or TF-links between 1-junctions adjoining added zero effort sources and 0-junctions adjoining added zero effort sources ($\boldsymbol{J}_3(\boldsymbol{x})$ is not identically equal to zero).

Since Algorithm 2 is applied in step 4 there are only P-links or TF-links between 0-junctions adjoining added zero flow sources and 1-junctions adjoining added zero flow sources ($\boldsymbol{J}_9(\boldsymbol{x})$ is not identically equal to zero). Also, there are only GY-links between 0-junctions adjoining added zero flow sources and added zero effort sources ($\boldsymbol{J}_6(\boldsymbol{x})$ is not identically equal to zero).

Since $\boldsymbol{e}_1^{\mathrm{Se}_0} = 0, \boldsymbol{e}_2^{\mathrm{Se}_0} = 0$, $\boldsymbol{f}_1^{\mathrm{Se}_0} = 0, \boldsymbol{f}_2^{\mathrm{Se}_0} = 0$ the added zero sources do not influence the interconnection relations of the ports belonging to Π. Therefore, we can eliminate all added zero sources, all auxiliary junctions and all basic links where one of edges is an auxiliary junction (step 5). As a result, an IOGJS described by

$$\begin{bmatrix} \boldsymbol{e}_1 \\ \boldsymbol{f}_2 \end{bmatrix} = -\boldsymbol{J}(\boldsymbol{x}) \begin{bmatrix} \boldsymbol{f}_1 \\ \boldsymbol{e}_2 \end{bmatrix}.$$

is obtained. Here, $\boldsymbol{J}(\boldsymbol{x})$ is a skew-symmetric matrix. The relations describing auxiliary variables are given by

$$\begin{aligned} \boldsymbol{f}_2^{\mathrm{Se}_0} &= \boldsymbol{J}_1(\boldsymbol{x})\begin{bmatrix}\boldsymbol{f}_1\\ \boldsymbol{e}_2\end{bmatrix} + \boldsymbol{J}_3(\boldsymbol{x})\boldsymbol{f}_1^{\mathrm{Se}_0} - \boldsymbol{J}_6^{\mathrm{T}}(\boldsymbol{x})\boldsymbol{e}_2^{\mathrm{Sf}_0} \\ \boldsymbol{e}_1^{\mathrm{Sf}_0} &= \boldsymbol{J}_2(\boldsymbol{x})\begin{bmatrix}\boldsymbol{f}_1\\ \boldsymbol{e}_2\end{bmatrix} - \boldsymbol{J}_9^{\mathrm{T}}(\boldsymbol{x})\boldsymbol{e}_2^{\mathrm{Sf}_0} \end{aligned} . \tag{21}$$

Remark 6 (*Deriving the Dirac structure from GJS*)

The relation (21) does not uniquely define the values of $\boldsymbol{f}_1^{\mathrm{Se}_0}$, $\boldsymbol{f}_2^{\mathrm{Se}_0}$, $\boldsymbol{e}_1^{\mathrm{Sf}_0}$, $\boldsymbol{e}_2^{\mathrm{Sf}_0}$. This is discussed in subsection 4.2.6.

Example 7 (*Continuation of Example 1*)

Consider the GBG shown in Figure $5b$. The Algorithm 3 is applied to the GJS of GBG shown in Figure $5b$. An extended IOBGB is shown in Figure 17 (step 1). The interconnection relations of extended IOGJS are given by (step 2)

$$\begin{bmatrix} e_2\\ e_6\\ \hdashline f_1\\ f_3\\ f_4\\ f_5 \end{bmatrix} = -\underbrace{\left[\begin{array}{cc:cccc} 0 & 0 & -1 & 1 & 0 & 0\\ 0 & 0 & 0 & 1 & -r & 0\\ \hdashline 1 & 0 & 0 & 0 & 0 & 0\\ -1 & -1 & 0 & 0 & 0 & 0\\ 0 & r & 0 & 0 & 0 & 1\\ 0 & 0 & 0 & 0 & -1 & 0 \end{array}\right]}_{\boldsymbol{J}^{\mathrm{ex}}} \begin{bmatrix} f_2\\ f_6\\ \hdashline e_1\\ e_3\\ e_4\\ e_5 \end{bmatrix}.$$

After applying steps 3 (ports π_3, π_6 interchange their positions) an equivalent extended IOGJS is obtained (Figure 18).

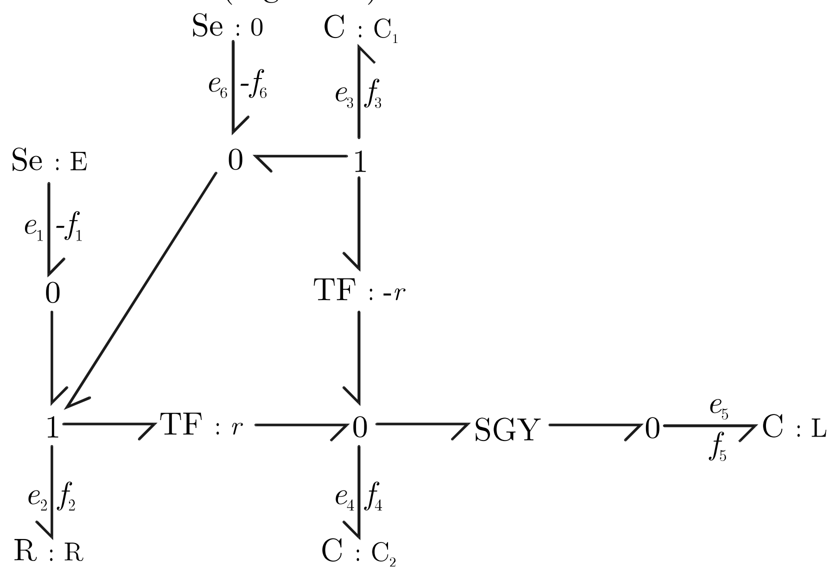

Figure 18: Extended equivalent IOGBG representation of GBG shown in Figure 17.

The interconnection relations are given by

$$\begin{bmatrix} e_2 \\ e_3 \\ \hline f_1 \\ f_6 \\ f_4 \\ f_5 \end{bmatrix} = -\left[\begin{array}{cc|cccc} 0 & 0 & -1 & -1 & r & 0 \\ 0 & 0 & 0 & 1 & -r & 0 \\ \hline 1 & 0 & 0 & 0 & 0 & 0 \\ 1 & -1 & 0 & 0 & 0 & 0 \\ -r & r & 0 & 0 & 0 & 1 \\ 0 & 0 & 0 & 0 & -1 & 0 \end{array}\right] \begin{bmatrix} f_2 \\ f_3 \\ \hline e_1 \\ e_6 \\ e_4 \\ e_5 \end{bmatrix}.$$

Since there are no added zero flow sources step 4 does not change anything. IOGJS obtained after applying step 5 is shown in Figure 19.

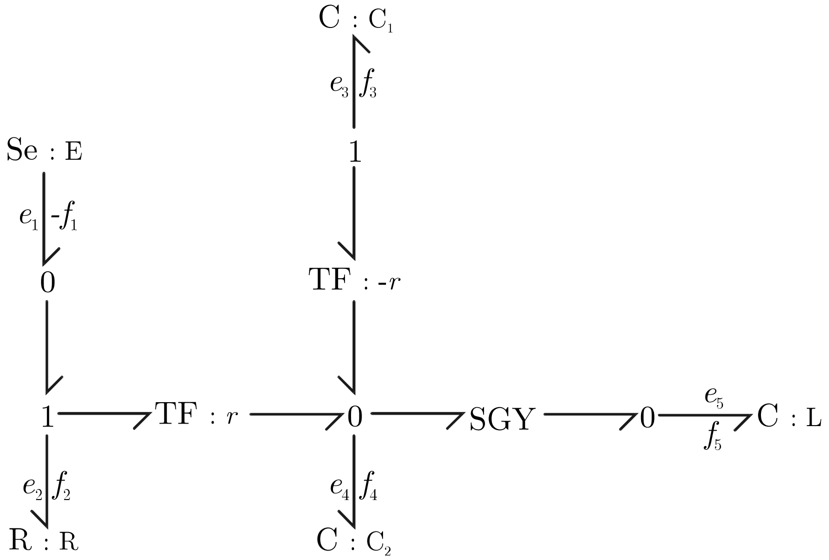

Figure 19: Equivalent IOGBG representation of GBG shown in Figure 17.

The interconnection relations are given by

$$\begin{bmatrix} e_2 \\ e_3 \\ \hline f_1 \\ f_4 \\ f_5 \end{bmatrix} = -\left[\begin{array}{cc|ccc} 0 & 0 & -1 & r & 0 \\ 0 & 0 & 0 & -r & 0 \\ \hline 1 & 0 & 0 & 0 & 0 \\ -r & r & 0 & 0 & 1 \\ 0 & 0 & 0 & -1 & 0 \end{array}\right] \begin{bmatrix} f_2 \\ f_3 \\ \hline e_1 \\ e_4 \\ e_5 \end{bmatrix}.$$

4.2.6. Singular GJS

Consider the electrical circuit shown in Figure $20a$. The (generalized) bond graph model of this system is shown in Figure $20b$. The equations describing the GJS shown in Figure $20b$ are given by $f_2 = f_1$, $e_2 = -e_1$, $e_p - e_g = e_1$. It is clear that we can not uniquely determine the values of the efforts of 0-junctions. The physical explanation is that we have not defined the ground of the circuit. If would set $e_g = 0$ then e_p would be uniquely defined. This type of generalized junction structure is called a singular GJS. The formal definition is given below.

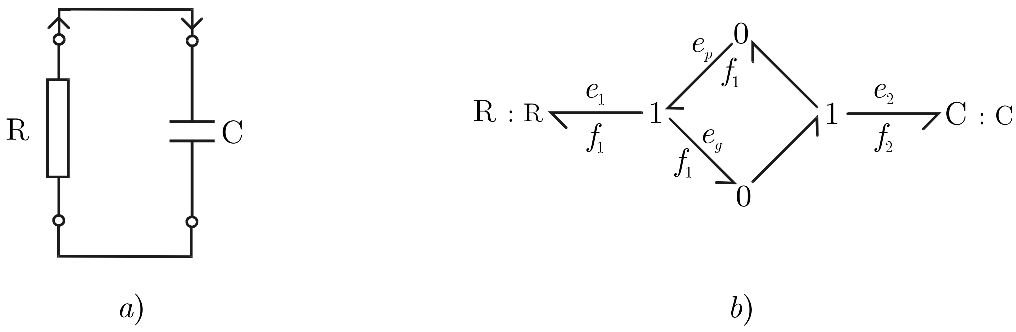

Figure 20: a) RC electrical circuit b) (generalized) bond graph model

Definition 16 (*Singular and non-singular generalized junction structure*)
Consider a GBG satisfying the conditions [As1a]-[As1e]. The generalized junction structure is called non-singular if $\forall \boldsymbol{x} \in \mathcal{X}$ *all internal variables are uniquely defined by the port variables. A GJS is called singular if it is not non-singular.*

In subsection 4.2.4 it has been shown how a GJS can be transformed into an extended IOGJS. If we know the values of the port variables of the extended IOGJS then the internal variables of the GJS are uniquely defined. Since the port variables of the extended IOGJS are the port variables of the GJS and the auxiliary variables, it follows that the internal variables of the GJS are uniquely defined by its port variables if and only if the auxiliary variables are uniquely defined by the port variables. This is summarized as follows.

Theorem 6 (*Non-singular generalized junction structure*)
Consider a GBG satisfying the conditions [As1a]-[As1e]. Let its GJS be transformed into an extended IOGJS. The generalized junction structure is non-singular if and only if $\forall \boldsymbol{x} \in \mathcal{X}$ *all auxiliary variables are uniquely defined by the port power variables of the GJS.*

Apply Algorithm 3 to a GJS without performing step 4. Then the relations describing the auxiliary variables are expressed by (21). The auxiliary variables $\boldsymbol{f}_2^{\mathrm{Se}_0}$, $\boldsymbol{e}_1^{\mathrm{Sf}_0}$ can be uniquely determined if and only if the matrices $\boldsymbol{J}_3(\boldsymbol{x})$, $\boldsymbol{J}_6(\boldsymbol{x})$ and $\boldsymbol{J}_9(\boldsymbol{x})$ are identically equal to zero. This means that there are no added zero flow sources adjoining the 0-junctions and no added zero effort sources adjoining the 1-junctions. In that case the relations describing the auxiliary variables are expressed by

$$\begin{bmatrix} \boldsymbol{f}^{\mathrm{Se}_0} \\ \boldsymbol{e}^{\mathrm{Sf}_0} \end{bmatrix} = \begin{bmatrix} \boldsymbol{J}_1(\boldsymbol{x}) \\ \boldsymbol{J}_2(\boldsymbol{x}) \end{bmatrix} \begin{bmatrix} \boldsymbol{f}_1 \\ \boldsymbol{e}_2 \end{bmatrix}.$$

This is summarized as follows.

Theorem 7 (*Non-singular generalized junction structure*)

Consider a GBG satisfying the conditions [As1a]-[As1e]. Assume that its GJS is transformed into an extended IOGJS. The generalized junction structure is non-singular if and only if for every $\boldsymbol{x} \in \mathcal{X}$ *there exists an IOGJS which is equivalent to the extended IOGJS such that all added zero effort sources adjoin 0-junctions and all added zero flow sources adjoin 1-junctions.*

Example 8: (*RC circuit shown in Figure 20*)

Consider the generalized bond graph shown in Figure 20b. Th extended IOGBG is shown in Figure 21a. After applying Algorithm 3 to the extended IOGJS shown in Figure 21a an equivalent extended IOGJS is obtained as shown in Figure 21b. Since there is an added zero flow source port adjoining a 0-junction, one can conclude that the GJS shown in Figure 20b is singular. However, the interconnection relations of ports belonging to Π are uniquely determined (encircled part shown in Figure 21b) as

$$\begin{bmatrix} e_1 \\ f_2 \end{bmatrix} = -\begin{bmatrix} 0 & 1 \\ -1 & 0 \end{bmatrix} \begin{bmatrix} f_1 \\ e_2 \end{bmatrix}.$$

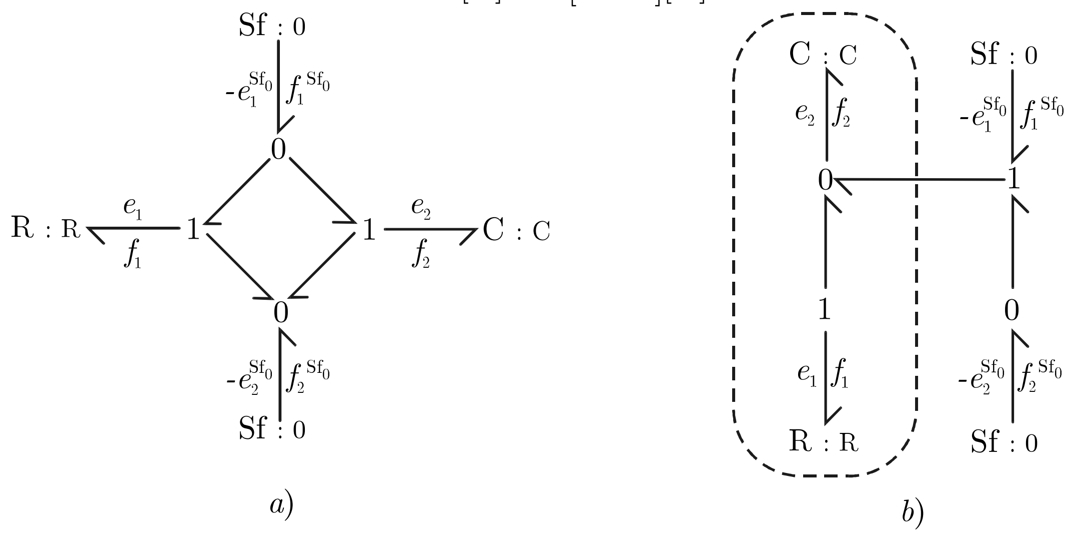

Figure 21: a) Extended IOGBG b) Equivalent extended IOGBG

Consider the case when the auxiliary variables can be uniquely determined only for the states in some subset $\mathcal{S}$ of $\mathcal{X}$. The values of $\boldsymbol{x}$ for which the auxiliary variable can not be uniquely determined are called the singular configurations of the considered system. This type of GJS often appears in GBG representing rigid bodies with closed chains (the internal power variables are usually the constraint forces in a joint).

5. Conclusion

The main contribution of this paper is given in section 4. It has been proved (Theorem 2) that a Dirac structure can be associated to every generalized junction structure. Also a constructive algorithm to obtain the Dirac structure has been given (Algorithm 3). The concept of a singular generalized junction structure has been introduced, and sufficient and necessary conditions for a generalized junction structure being non-singular have been given. Also, the transformation of a singular bond graph into a non-singular one has been treated. The tools developed in subsection 4.2 (Algorithm 2) are the basis for the further analysis of the generalized bond graph and the extraction of equations suitable for numerical simulation, as will be dealt with in the second part of this paper.

Literature

[1] C. Bidard, *Displaying Kirchhoff's invariants in Simple Junction Structures*, in P. C. Breedveld and G. Dauphin-Tanguy, eds., *13th IMACS World Congress*, North Holland / Elsevier, Dublin, 1991, pp. 1064-1068.

[2] S. H. Birkett and P. H. Roe, *The Mathematical Foundations of Bond graphs - I. Algebraic Theory*, Journal of the Franklin Institute, 326 (1989), pp. 329-350.

[3] S. H. Birkett and P. H. Roe, *The Mathematical Foundations of Bond graphs - II. Duality*, Journal of the Franklin Institute, 326 (1989), pp. 691-708.

[4] S. H. Birkett and P. H. Roe, *The Mathematical Foundations of Bond graphs - III. Matroid Theory*, Journal of the Franklin Institute, 327 (1990), pp. 87-108.

[5] S. H. Birkett and P. H. Roe, *The Mathematical Foundations of Bond graphs - IV. Matrix Representations and Causality*, Journal of the Franklin Institute, 327 (1990), pp. 109-128.

[6] A. M. Bloch and P. E. Crouch, *Representation of Dirac Structure on Vector Spaces and Nonlinear L-C circuits*, in G. Ferreyra, R. Gardner, H. Hermes and H. Sussmann, eds., *Symposia in pure Mathematics, Differential Geometry and Control Theory, AMS, 1999*, 1999, pp. 103-117.

[7] P. C. Breedveld, *Decomposition of Multiport Elements in a Revised Multibond Graph Notation*, Journal of the Franklin Institute, 318 (1984), pp. 253-273.

[8] P. C. Breedveld, *Multibond Graph Elements in Physical System Theory*, Journal of the Franklin Institute, 319 (1985), pp. 1-36.

[9] P. C. Breedveld, *Physical Systems Theory in Terms of Bond Graphs*, Ph.D. Thesis, *Electrical Engineering*, Twente, Enschede, 1984, pp. 201.

[10] P. C. Breedveld, *Thermodynamic Bond Graphs and the Problem of Thermal Inertance*, Journal of the Franklin Institute, 314 (1984), pp. 15-40.

[11] T. J. Courant, *Dirac Manifolds*, Transactions of the American Mathematical Society, 319

(1990), pp. 631-661.

[12] M. Dalsmo and A. J. van der Schaft, *On Representations and Integrability of Mathematical Structures in Energy-Conserving Physical Systems*, SIAM Journal on Control and Optimization, 37 (1999), pp. 54-91.

[13] D. C. Karnopp, D. L. Margolis and R. C. Rosenberg, *Systems Dynamics: A Unified Approach*, John Wiley, New York, 1990.

[14] J. D. Lamb, D. R. Woodall and G. M. Asher, *Bond graphs I: Acausal Equivalence*, Discrete Applied Mathematics, 72 (1997), pp. 261-293.

[15] J. D. Lamb, D. R. Woodall and G. M. Asher, *Bond graphs II: Causality and Singularity*, Discrete Applied Mathematics, 73 (1997), pp. 143-173.

[16] J. D. Lamb, D. R. Woodall and G. M. Asher, *Bond graphs III: Bond Graphs ans Electrical Networks*, Discrete Applied Mathematics, 73 (1997), pp. 211-250.

[17] J. D. Lamb, D. R. Woodall and G. M. Asher, *Equivalences of Bond Graph Junction Structures*, , *ICBGM'93*, San Diego, California, 1993, pp. 79-84.

[18] B. Maschke, A. J. van der Schaft and P. C. Breedveld, *An Intrinsic Hamiltonian Formulation of Network dynamics: Non-Standard Poisson Structures and Gyrators*, Journal of the Franklin Institute, 329 (1992), pp. 923-966.

[19] B. M. Maschke, R. Ortega and A. J. van der Schaft, *Energy-Based Lyapunov Functions for Forced Hamiltonian Systems with Dissipation*, Internal report, University of Twente, Faculty of Mathematical Sciences, Enschede, 1998, pp. 1-16.

[20] H. Nijmeijer and A. J. van der Schaft, *Nonlinear Dynamical Control Systems*, Springer-Verlag, New York, 1996.

[21] G. F. Oster and A. S. Perelson, *Chemical Reaction Dynamics Part I: Geometrical Structure*, Archive of Rational Mech. Anal., 57 (1975), pp. 230-274.

[22] H. M. Paynter, *Analysis and Design of Engineering Systems*, The M.I.T. Press, Cambridge, Massachusetts, 1961.

[23] A. S. Perelson, *Bond Graph Junction Structure*, Journal of Dynamic Systems, measurement and Control, Transactions ASME, Series G, 96 (1975), pp. 189-195.

[24] A. S. Perelson and G. F. Oster, *Chemical Reaction Dynamics Part II: Reaction Networks*, Archive of Rational Mech. Anal., 55 (1975), pp. 31-98.

[25] A. S. Perelson and H. M. Paynter, *Discussion "The Properties of Bond Graph Junction Structure Matrices"*, Journal of Dynamic Systems, measurement and Control, Transactions ASME, Series G, 95 (1976), pp. 209-210.

[26] R. C. Rosenberg and J. R. Andry, *Solvability of Bond Graphs Junction Structures with Loops*, IEEE Transactions on Circuit and Systems, CAS-26 (1979), pp. 130-137.

[27] R. C. Rosenberg and B. Moultrie, *Basis Order for Bond Graph Junction Structures*, IEEE Transactions on Circuit and Systems, CAS-27 (1980), pp. 909-920.

[28] A. J. van der Schaft, *Interconnection and Geometry*, in J. W. Polderman and H. L. Trentelman, eds., *The Mathematics of Systems and Control: From Intelligent Control to Behaviour Systems*, 1999, pp. 203-218.

[29] A. J. van der Schaft, M. Dalsmo and B. M. Maschke, *Mathematical Structures in the Network Representation of Energy-Conserving Physical Systems*, , University of Twente, Faculty of

Mathematical Sciences, Enschede, 1996, pp. 1-7.
[30] A. J. van der Schaft and B. M. Maschke, *The Hamiltonian Formulation of Energy Conserving Physical Systems with External Ports*, Archiv fur Elektronik und Ubertragungstechnik, 49 (1995), pp. 362-371.
[31] A. J. van der Schaft and B. M. Maschke, *On the Hamiltonian Formulation of Nonholonomic Mechanical Systems*, Reports on Mathematical Physics, 34 (1994), pp. 225-232.
[32] J. van Dijk, *On the Role of Bond Graph Causality in Modelling Mechatronic Systems*, , *Faculty of Electrical Engineering*, Twente, Enschede, 1994, pp. 221.

Appendix 1 (the proofs of Theorem 3, Theorem 4, Theorem 5)

Proof of Theorem 3

Let $\mathcal{D}$ denote a Dirac structure related to $\mathbb{IOGJS}$. $\mathcal{D}$ is represented in kernel form as

$$\left[\boldsymbol{E}(\boldsymbol{x}) \mid \boldsymbol{F}(\boldsymbol{x})\right]\begin{bmatrix}\boldsymbol{e} \\ \hdashline \boldsymbol{f}\end{bmatrix} = 0\,. \tag{22}$$

By applying the partial dualization procedure to π_i the power variable e_i, f_i interchange positions, and (22) can be rewritten as

$$0 = \left[\boldsymbol{E}(\boldsymbol{x}) \mid \boldsymbol{F}(\boldsymbol{x})\right]\boldsymbol{Q}^{\mathrm{T}}_{i\leftrightarrow n+i}\boldsymbol{Q}_{i\leftrightarrow n+i}\begin{bmatrix}\boldsymbol{e} \\ \hdashline \boldsymbol{f}\end{bmatrix} = \left[\bar{\boldsymbol{E}}(\boldsymbol{x}) \mid \bar{\boldsymbol{F}}(\boldsymbol{x})\right]\begin{bmatrix}\bar{\boldsymbol{e}} \\ \hdashline \bar{\boldsymbol{f}}\end{bmatrix}. \tag{23}$$

Here, $\boldsymbol{Q}_{i\leftrightarrow n+i}$ is an $2n$-dimensional permutation matrix that interchanges the positions i and $i+n$. The relation (23) represents a Dirac structure, denoted by $\bar{\mathcal{D}}$. Indeed, the rank condition is satisfied since

$$\mathrm{rank}\left(\left[\bar{\boldsymbol{E}}(\boldsymbol{x}) \mid \bar{\boldsymbol{F}}(\boldsymbol{x})\right]\right) = \mathrm{rank}\left(\left[\boldsymbol{E}(\boldsymbol{x}) \mid \boldsymbol{F}(\boldsymbol{x})\right]\boldsymbol{Q}^{\mathrm{T}}_{i\leftrightarrow n+i}\right) = n\,,$$

and the power conservation condition is satisfied since

$$\begin{aligned}&\bar{\boldsymbol{E}}(\boldsymbol{x})\bar{\boldsymbol{F}}^{\mathrm{T}}(\boldsymbol{x}) + \bar{\boldsymbol{F}}(\boldsymbol{x})\bar{\boldsymbol{E}}^{\mathrm{T}}(\boldsymbol{x}) = \\ &\boldsymbol{E}(\boldsymbol{x})\boldsymbol{Q}^{\mathrm{T}}_{i\leftrightarrow n+i}\boldsymbol{Q}_{i\leftrightarrow n+i}\boldsymbol{F}^{\mathrm{T}}(\boldsymbol{x}) + \boldsymbol{F}(\boldsymbol{x})\boldsymbol{Q}^{\mathrm{T}}_{i\leftrightarrow n+i}\boldsymbol{Q}_{i\leftrightarrow n+i}\boldsymbol{E}^{\mathrm{T}}(\boldsymbol{x}) = \\ &\boldsymbol{E}(\boldsymbol{x})\boldsymbol{F}^{\mathrm{T}}(\boldsymbol{x}) + \boldsymbol{F}(\boldsymbol{x})\boldsymbol{E}^{\mathrm{T}}(\boldsymbol{x}) = 0.\end{aligned}$$

Also, $\mathcal{D}$ and $\bar{\mathcal{D}}$ are equivalent on the whole sate space $\mathcal{X}$ $(\boldsymbol{K} = \mathrm{I}_n, \boldsymbol{Q} = \boldsymbol{Q}_{i,\leftrightarrow n+i})$. Assume without loss of generality that the partial dualization procedure is applied to a port π_i adjoining an 1-junction. The Dirac structure $\bar{\mathcal{D}}$ can be represented in a hybrid input-output form where $\bar{\boldsymbol{E}}_1(\boldsymbol{x})$ is obtained from the matrix $\boldsymbol{E}_1(\boldsymbol{x})$ (the first

n_1 columns of the matrix $\boldsymbol{E}(\boldsymbol{x})$) by removing its i^{th} column and $\bar{\boldsymbol{F}}_2(\boldsymbol{x})$ is obtained by adding the i^{th} column of $\boldsymbol{E}_1(\boldsymbol{x})$ (after partial dualization this column belongs to $\bar{\boldsymbol{F}}(\boldsymbol{x})$) to the matrix $\boldsymbol{F}_2(\boldsymbol{x})$ (the last n_2 columns of the matrix $\boldsymbol{F}(\boldsymbol{x})$). Then it is clear that $\operatorname{rank}\left[\bar{\boldsymbol{E}}_1(\boldsymbol{x}) \,\vdots\, \bar{\boldsymbol{F}}_2(\boldsymbol{x})\right] = n$. This hybrid input-output representation, denoted by $\mathcal{D}_{\text{eq}}$ ($\mathcal{D}_{\text{eq}} \equiv \bar{\mathcal{D}}$ on $\mathcal{X}$), can be related to an IOGJS denoted by $\mathbb{IOGJS}_{\text{eq}}$. From the construction of the matrix $\bar{\boldsymbol{F}}_2(\boldsymbol{x})$ it is clear that the dualized port $\bar{\pi}_i$ adjoins a 0-junction. Since $\mathcal{D}_{\text{eq}} \equiv \bar{\mathcal{D}}$ and $\mathcal{D}$ and $\bar{\mathcal{D}}$ are equivalent on $\mathcal{X}$, $\mathcal{D}_{\text{eq}}$ is equivalent to $\mathcal{D}$ on $\mathcal{X}$. Hence, $\mathbb{IOGJS} \underset{\mathcal{X}}{\sim} \mathbb{IOGJS}_{\text{eq}}$. ■

Proof of Theorem 4

Let $\mathcal{D}$ denote a Dirac structure related to $\mathbb{IOGJS}$. $\mathcal{D}$ is represented in kernel form (22). It is clear that $\left[\boldsymbol{E}_1(\boldsymbol{x}) \,\vdots\, \boldsymbol{F}_2(\boldsymbol{x})\right] = \boldsymbol{I}_n$ (see (12)). The matrix $\bar{\boldsymbol{E}}_1(\boldsymbol{x})$ is obtained from the matrix $\boldsymbol{E}_1(\boldsymbol{x})$ by replacing its i^{th} column with the j^{th} column of the matrix $\boldsymbol{E}_2(\boldsymbol{x})$. Similarly, $\bar{\boldsymbol{F}}_2(\boldsymbol{x})$ is obtained from the matrix $\boldsymbol{F}_2(\boldsymbol{x})$ by replacing its j^{th} column with the i^{th} column of the matrix $\boldsymbol{F}_1(\boldsymbol{x})$. Then,

$$\left[\bar{\boldsymbol{E}}_1(\boldsymbol{x}) \,\vdots\, \bar{\boldsymbol{F}}_2(\boldsymbol{x})\right] = \begin{bmatrix} 1 & \cdots & 0 & * & 0 & \cdots & 0 & * & 0 & \cdots & 0 \\ \vdots & \ddots & \vdots & \vdots & \vdots & \ddots & \vdots & \vdots & \vdots & \ddots & \vdots \\ 0 & \cdots & 1 & * & 0 & \cdots & 0 & * & 0 & \cdots & 0 \\ 0 & \cdots & 0 & r(x) & 0 & \cdots & 0 & 0 & 0 & \cdots & 0 \\ 0 & \cdots & 0 & * & 1 & \cdots & 0 & * & 0 & \cdots & 0 \\ \vdots & \ddots & \vdots & \vdots & \vdots & \ddots & \vdots & \vdots & \vdots & \ddots & \vdots \\ 0 & \cdots & 0 & * & 0 & \cdots & 1 & * & 0 & \cdots & 0 \\ 0 & \cdots & 0 & 0 & 0 & \cdots & 0 & -r(x) & 0 & \cdots & 0 \\ 0 & \cdots & 0 & * & 0 & \cdots & 0 & * & 1 & \cdots & 0 \\ \vdots & \ddots & \vdots & \vdots & \vdots & \ddots & \vdots & \vdots & \vdots & \ddots & \vdots \\ 0 & \cdots & 0 & * & 0 & \cdots & 0 & * & 0 & \cdots & 1 \end{bmatrix}.$$

Therefore, $\det\left[\bar{\boldsymbol{E}}_1(\boldsymbol{x}) \,\vdots\, \bar{\boldsymbol{F}}_2(\boldsymbol{x})\right] = -r^2(x)$. Hence, $\operatorname{rank}\left[\bar{\boldsymbol{E}}_1(\boldsymbol{x}) \,\vdots\, \bar{\boldsymbol{F}}_2(\boldsymbol{x})\right] = n, \forall \boldsymbol{x} \in \mathcal{S}$. This means that we can find a hybrid input-output representation $\mathcal{D}_{\text{eq}}$ equivalent to $\mathcal{D}$ on $\mathcal{S}$. This Dirac structure $\mathcal{D}_{\text{eq}}$ can be related to an IOGJS, denoted by $\mathbb{IOGJS}_{\text{eq}}$. From the construction of the matrices $\bar{\boldsymbol{E}}_1(\boldsymbol{x})$, $\bar{\boldsymbol{F}}_2(\boldsymbol{x})$ it is clear that π_i adjoins a 0-junction and π_{n_1+j} adjoins a 1-junction. Since, $\mathcal{D}_{\text{eq}}$ is equivalent to $\mathcal{D}$ on $\mathcal{S}$ it follows that $\mathbb{IOGJS} \underset{\mathcal{S}}{\sim} \mathbb{IOGJS}_{\text{eq}}$. An extensive but straightforward analysis shows that there is a TF-link $\left(\chi_i^1, \tau^{\text{TF}}, \chi_j^0\right)$ with the ratio of transformer being $r^{-1}(\boldsymbol{x})$. ■

Proof of Theorem 5

Assume without loss of generality that the reconnecting procedure via a gyrator is applied to π_i, π_j adjoining 1-junctions χ_i^1, χ_j^1, respectively and $i < j$. Firstly, apply the partial dualization procedure to π_j. An equivalent IOGJS is obtained where $\overline{\pi}_j$ adjoins a 0-junction $\chi_{n_2+1}^0$ and there is a TF-link $\left(\chi_i^1, \tau^{\mathrm{TF}}, \chi_{n_2+1}^0\right)$ with the ratio of the transformer equal to $r(\boldsymbol{x})$. Secondly, apply the reconnecting procedure via a transformer on π_i and $\overline{\pi}$. An equivalent IOGJS is obtained where π_i, $\overline{\pi}$ adjoin $\chi^0_{\ 2+1}$, χ_i^1, respectively. Also there is a TF-link $\left(\chi_i^1, \tau \ , \chi_{\ 2+1}\right)$ with the ratio of the transformer equal to $r^{-1}(\boldsymbol{x})$. Thirdly, apply again a partial dualization procedure to $\overline{\pi}$. An equivalent IOGJS is obtained where $\overline{\overline{\pi}}_j = \pi_j$ adjoins a 0-junction $\chi_{n_2+2}^0$ and there is a GY-link $\left(\chi_{\ 2+1}, \tau^{\mathrm{GY}}, \chi_{\ 2+2}\right)$ with the ratio of the gyrator $r^{-1}(\boldsymbol{x})$. ■